

# Rate of epidemic spreading on complex networks

Samuel Cure<sup>1</sup>, Florian G. Pflug<sup>1</sup>, and Simone Pigolotti<sup>1\*</sup>

<sup>1</sup>*Biological Complexity Unit, Okinawa Institute of Science and Technology, Onna, Okinawa 904-0495, Japan.*

<sup>\*</sup>*simone.pigolotti@oist.jp*

June 26, 2024

---

## Abstract

The initial phase of an epidemic is often characterised by an exponential increase in the number of infected individuals. In a well-mixed population, this exponential increase is controlled by the basic reproduction number  $R_0$  and the distribution of times between consecutive infection along an infection chain. However, real populations are characterised by a complex network of interactions, and are thus far from being well mixed. Here, we derive an expression for the rate of exponential spread of an epidemic on a complex network. We find that this rate is affected by the degree distribution, the network assortativity, and the level of clustering. Our result holds for a broad range of networks, apart from networks with very broad degree distribution, where no clear exponential regime is present. The theory presented in this paper bridges the gap between classic epidemiology and the theory of complex network, with broad implications for model inference and policy making.

---

Epidemic modelling permits rationalisation of evidences and can provide crucial information for policy making. Epidemiological models should incorporate the key features that determine epidemic spreading. One such feature is the arrangement of individuals in social structures [1]. These social structures play a crucial role in the spreading of an epidemic, and in the effectiveness of intervention strategies [2, 3]. In these social structures, the number of contacts per individual is highly variable. For example, at the early stages of COVID-19, the individuals with most contacts contributed disproportionately to the epidemic [4, 5].

A convenient way of modelling social structures is by means of complex networks [6], in which nodes represent individuals and links signify pairs of individuals that are in close contact. A success of network theory has been to determine the epidemic threshold on networks [7, 8, 9], i.e., the transition point from a localised outbreak to a widespread epidemic. This theory has shown that networks whose degree distribution has a diverging variance due to heavy tails [7, 10, 9] are extremely vulnerable to epidemics. A paradigmatic example is found in the Barabási-Albert model [11], where a network is constructed by preferentially attaching new nodes to existing nodes with high degree. Another property of complex

networks which is relevant for epidemic spreading is clustering, which is a measure of how commonly nodes tend to form tightly connected communities. Many networks in nature possess both fat tails in their degree distribution and high level of clustering [12].

Another key feature of an epidemic is its infectiousness, i.e., the rate at which an infected individual infects its contacts. The infectiousness incorporates multiple factors, such as the viral load of an individual, its social behaviour, and possibly environmental factors [13]. Because of changes in these factors, the infectiousness of an individual tends to change in time in a way that is particular to each disease. This time-dependence profoundly impacts the way a disease spreads.

Social structures and individual infectiousness are the key factors in determining the initial stage of an epidemic, in which most individuals are susceptible and the number of infected individuals usually grows exponentially. This stage is of central importance for novel epidemics, or during emergence of novel variants, and it often requires rapid policy making. At later stages, other factors become relevant, such as individual recovery time, their behavioural change as a consequence of the epidemic [14], and the possible occurrence of reinfections.

Despite the vast body of theory on epidemics in networks [9], general results on the speed of epidemic spreading are surprisingly sparse. The rate of epidemic spreading can be calculated for unclustered, uncorrelated networks, and with constant infectiousness [15]. A recent theory estimates the average time it takes for an epidemic to reach an individual at a certain distance from patient zero [16]. The spread of an epidemic on a network can be exactly solved [17], but this calculation becomes practically unfeasible unless the network is very small. Other approaches avoid a detailed description of social structures, and effectively model the heterogeneity of the population by assigning different risk propensities to individuals [18, 19].

In this paper, we present a general theory that predicts the exponential rate of epidemic spreading on a complex network. In particular, we quantify the impact of key properties of the network, such as assortativity and clustering, on the reproduction number of the epidemic. We further link the reproduction number and the individual infectiousness with the epidemic spreading rate. We shall see that this approach leads to accurate predictions for a broad range of networks.

## Epidemic spreading in well-mixed populations

We begin by summarising classic results of epidemic modelling in well-mixed populations [13]. In this case, the cumulative number  $I(t)$  of infected individuals at time  $t$  is governed by the renewal equation

$$\dot{I}(t) = \int_0^t d\tau R_0 w(\tau) \dot{I}(t - \tau), \quad (1)$$

where the basic reproduction number  $R_0$  represents the average number of secondary infections by each infected individual, and the dot denotes a time derivative. The function  $w(\tau)$  is the infectiousness, defined as the probability density that a given secondary infection occurs after a time  $\tau$  from the primary one. We assume to be in the exponential regime,  $I(t) \sim e^{\Lambda t}$ , where  $\Lambda$  is the rate of exponential spread. Substituting this assumption into Eq. (1) and taking the limit of large time, we obtain the Euler-Lotka equation

$$\frac{1}{R_0} = \langle e^{-\Lambda \tau} \rangle, \quad (2)$$

where the average  $\langle \dots \rangle$  is over the distribution  $w(\tau)$ . Equation (2) is a cornerstone in mathematical epidemiology, as it provides a fundamental link between the three key quantities governing the epidemic spreading: the distribution of infection times  $w(\tau)$ ; the basic reproduction number  $R_0$ ; and the exponential spreading rate  $\Lambda$ .

## Epidemic spreading in networks.

We now consider a structured population composed of  $N$  individuals, who are represented as nodes on a network (Fig. 1a). Two individuals are connected by a link if they are in contact, meaning that they can potentially infect one another. Once an individual is infected, it can spread the disease to each of its neighbours at rate  $\lambda(\tau)$ , where  $\tau$  is the time since the considered individual was infected. The probability that the individual infects a given neighbour at time  $\tau$ , given that the neighbour has not been infected before by someone else, is then equal to  $\psi(\tau) = \lambda(\tau) \exp[-\int_0^\tau \lambda(\tau') d\tau']$ . We call  $\psi(\tau)$  the generation time distribution (Fig. 1b). The integral  $p_\psi = \int_0^\tau \psi(\tau') d\tau'$  represents the total probability of infecting a susceptible neighbour. Aside from this normalisation, the generation time distribution plays the role of the distribution  $w(\tau)$  for well-mixed systems. In the following, we focus for simplicity on the case  $p_\psi = 1$ . In this case, individuals infect all of their contacts and the epidemic eventually spreads through all the network, if the network is connected. Our results can be extended to the case  $p_\psi < 1$  by randomly removing links in the networks (see Section I in SI).

Infected nodes cannot get reinfected and are never formally considered as recovered, although their infectiousness may wane over time. Our model can therefore be seen as a Susceptible-Infected model on a network with non-Markovian infection times. The Markov property only holds in the limiting case of constant  $\lambda(\tau)$ , and consequently exponentially distributed  $\psi(\tau)$ . This limiting case is often unrealistic. For example, the infectiousness of COVID-19 markedly increases for 3–6 days and then decay for about 11 days [20], and is therefore poorly described by an exponential distribution.

In the course of the epidemic, the number of infected rapidly grows before saturating (Fig. 1c). An alternative to the temporal perspective is to represent the epidemic in generations (Fig. 1d). We call  $Z_n$ ,  $n = 0, 1, \dots$  the average number of infected individuals in the  $n$ th generation. The initial generation,  $n = 0$ , is constituted by the patient zero,  $Z_0 = 1$ . In this representation, the infected individuals form a tree (Fig. 1e).

## Reproduction number on a complex network

The basic reproduction number  $R_0$  for a network is the average number of links of an infected individual in the early stage of the epidemic, excluding the one from which the infection came from. We also define the effective reproduction number  $R$  as the average number of infections caused by an infected individual. In contrast with  $R_0$ ,  $R$  does not include contacts that are infected by other individuals. This difference is crucial in clustered networks.

Our initial goal is to estimate  $R$  for a complex network. To this aim, we characterise individuals by their degree  $k$ . We introduce the reproduction matrix  $M_{kk'}$ , whose elements are the average numbers of susceptible individuals of degree  $k$  connected to a node of degree  $k'$ . The reproduction matrix is expressed by

$$M_{kk'} = (k' - 1 - m_{kk'})P(k|k') \quad (3)$$

where  $P(k|k')$  is the probability that a neighbour of a node of degree  $k'$  has degree  $k$  and  $m_{kk'}$  is the average number of triangles a  $kk'$ -link is part of. The term proportional to  $m_{kk'}$  in Eq. (3) discounts for contacts of a given individual that were already infected by someone else, due to the presence of triangles in the network. In Eq. (3), we neglect higher order loops such as squares. The reproductive matrix given in Eq. (3) has been used to study percolation on networks [21].

On the one hand, assuming that  $R$  remains constant between generations, the average number of infected individuals at the  $n$ th generation is equal to  $Z_n \sim R^n$ , up to the leading order. On the other hand, the number of infected individuals  $Z_n$  scales as the  $n$ -th power of the reproduction matrix (see Methods). This permits us to identify  $R$  as the leading eigenvalue of the reproduction matrix. The associated right eigenvector  $v_{k'}$  can be interpreted as the degree distribution

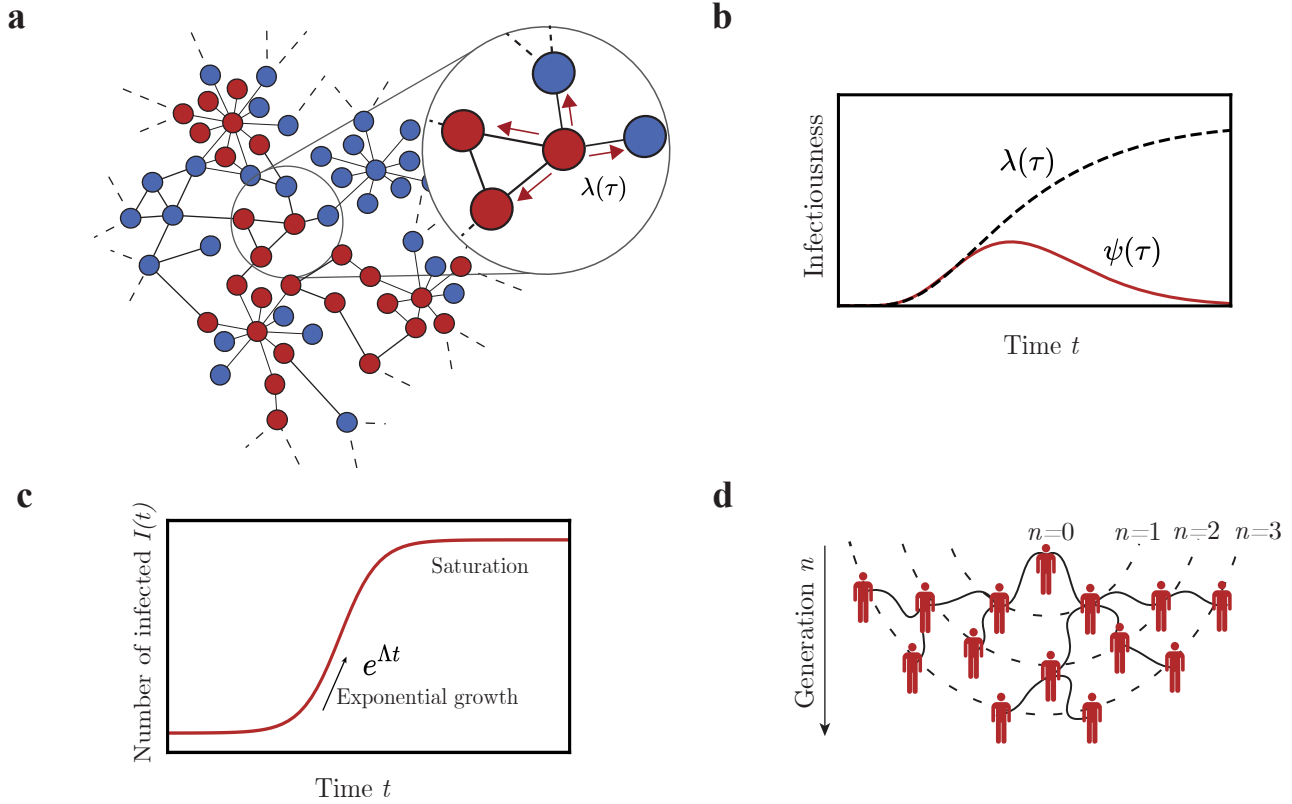


Figure 1: **Epidemic spreading on complex networks.** **a:** Epidemic on a network. Individuals (nodes) can be infected (red) or healthy (blue). Infected individuals spread the infection at a rate  $\lambda(\tau)$  to each of their neighbours, to whom they are connected via links. Individuals may have different numbers of neighbours. Due to the presence of cycles, some neighbours may have already been infected by someone else, so that the transmission does not result in an infection. **b:** Infected individuals spread the disease at a time-dependent rate  $\lambda(\tau)$ , where  $\tau$  is the time since they were infected. The resulting infection times are distributed according to  $\psi(\tau)$ . **c:** Example of an epidemic trajectory starting with one infected individual. After an outbreak, the epidemic spreads at an exponential spreading rate  $\Lambda$ . The exponential phase ends in a saturation phase, where a sizeable fraction of the individuals are already infected. **d:** Epidemic tree. The epidemic starts with a first infected individual (patient zero) and resulting infections are represented by continuous lines. Dashed lines represents different generations.

of the infected individuals (see Methods).

For large networks, diagonalising the reproduction matrix can be unwieldy. In the simple case of an unclustered network ( $m_{kk'} = 0$  for all links) in which the degrees of connected nodes are uncorrelated, we have

$$R = R_0 = \frac{\overline{k^2} - \bar{k}}{\bar{k}}, \quad (4)$$

where the bar represents an average over the degree distribution. Equation (4) is a classic result for epidemic spreading on networks [7, 22, 8]. We seek to extend it to the general case of clustered and correlated networks. We quantify degree correlations by the assortativity coefficient  $r$  (see Methods). When  $r > 0$ , nodes with high degree tend to connect together whereas when  $r < 0$ , they tend to connect to lower degree nodes. We find that, for small clustering coefficients and degree correlation, the effective reproduction number  $R$  is expressed by

$$R_{\text{pert}} = (1 - r)(R_0 - m_1) + \frac{r}{R_0 - m_1} \left( \frac{\overline{k(k-1)^2}}{\bar{k}} - 2m_2 + m_1^2 \right), \quad (5)$$

Table 1: **Effect of clustering and assortativity on the reproduction number.**

Network	$R_0$	$R$	$R_{\text{pert}}$	$R_{\text{pert}}^{(r=0)}$	$R_{\text{pert}}^{(\bar{c}=0)}$	Assortativity $r$	Clustering $\bar{c}$
BA <sub>1</sub>	13.9	8.5	6.8	13.9	6.6	-0.011	0
BA <sub>2</sub>	20.4	15.5	14.4	20.3	14.2	-0.008	0.0001
BA <sub>12</sub>	85.4	80.8	79.5	83.6	80.4	-0.004	0.0003
ER <sub>6</sub>	6.0	6.0	6.0	6.0	6.0	0.001	0.000
ER <sub>10</sub> $\alpha = 0.2$	10.0	9.0	9.1	9.0	10.7	0.062	0.108
WS <sub>8,2</sub>	7.2	4.9	4.9	4.9	7.0	-0.022	0.334
WS <sub>6,2</sub>	5.2	3.6	3.6	3.6	5.0	-0.029	0.315
LN <sub>4,1</sub> $\alpha = 0.5$	3.7	3.2	3.2	3.2	3.8	0.007	0.161

Parameters associated with the epidemic spreading for different models of complex networks. The basic reproduction number  $R_0$  is given by Eq. (4). The effective reproduction number  $R$  is the numerically computed leading eigenvalue of Eq. (3). We compare it with the analytical expression of  $R_{\text{pert}}$  given in Eq. (5). To assess the impact of degree correlations and clustering, we also compute  $R_{\text{pert}}$  for  $r = 0$  and for  $\bar{c} = 0$ , where we have defined  $\bar{c} = \sum_k c_k P(k)$ . BA <sub>$m$</sub> : Barabási-Albert model with parameter  $m$ . ER <sub>$d$</sub> : Erdős-Rényi with mean degree  $d$ . WS <sub>$k,p$</sub> : Watts-Strogatz starting from a 1D lattice with  $k$  nearest neighbours and rewiring probability  $p$ . LN<sub>4,1</sub>  $\alpha = 0.5$  is generated from a modified version of the configuration model [24] with a Lognormal degree distribution with mean 4 and variance 1. This modified algorithm allows us for tuning the clustering coefficients as  $c_k \propto (k-1)^{-\alpha}$  for a chosen  $\alpha > 0$ . ER<sub>10</sub>  $\alpha = 0.2$ : A Erdős-Rényi network in which we imposed clustering using the same algorithm.

where  $c_k$  is the probability that two neighbours of a node of degree  $k$  are themselves connected,  $m_1 = \overline{k(k-1)c_k/\bar{k}}$  is the average number of triangles a link is part of, and  $m_2 = \overline{k(k-1)^2c_k/\bar{k}}$ . Equation (5) is obtained by a perturbative expansion in  $r$  (see Methods).

We compare the expression for  $R_{\text{pert}}$  given in Eq. (5) to the maximum eigenvalue  $R$  of the matrix  $M_{kk'}$  for different network models, see Table 1. We find that the relative difference between  $R$  and  $R_{\text{pert}}$  is within 2% for all the networks we considered, except for Barabási-Albert with  $m = 1$  (20.6%) and  $m = 2$  (7.1%). We shall analyse the reason for this discrepancy later in the paper. Approximating  $R$  with  $R_0$  given in Eq. (4) leads to substantially larger errors, supporting that clustering and assortativity need to be taken into account to appropriately estimate  $R$ . Here and in the following, when computing  $R_{\text{pert}}$  using Eq. (5) and  $R_0$  using Eq. (4) for a given network, we always interpret the averages as empirical averages. With this choice, moments of the degree distribution are always finite, even in very heterogeneous networks. In practical cases, Eq. (5) predicts that the reproduction number  $R_{\text{pert}}$  increases with the assortativity  $r$ . Accordingly, assortativity lowers the epidemic threshold, as previously known for the unclustered case [23]. However, the coefficient multiplying  $r$  in Eq. (5) is usually rather small, except when the degree distribution has heavy tails. In contrast, clustering systematically reduces  $R_{\text{pert}}$ , regardless of the degree distribution. For this reason, we find that  $R_0$  overestimates  $R$  in all the synthetic networks we considered.

## Network Euler-Lotka equation

We now use our estimate of the reproduction number to predict how epidemics spread. The average total number  $I_k(t)$  of infected individual of degree  $k$  at time  $t$  is governed by the renewal equation

$$\dot{I}_k(t) = \sum_{k'} \int_0^t \dot{I}_{k'}(t-\tau) M_{kk'} \psi(\tau) d\tau. \quad (6)$$

Equation (6) extends Eq. (1) to complex networks. It is linear because of the assumption that the epidemic is in the initial stage and thus far from saturation. We assume exponential growth,  $\dot{I}_{k'}(u) \propto v_{k'} e^{\Lambda t}$ . Substituting this assumption into Eq. (6) we obtain, for large time,

$$\frac{1}{R} = \langle e^{-\Lambda \tau} \rangle, \quad (7)$$

where  $\langle \dots \rangle$  denotes an average over  $\psi(\tau)$ . We call Eq. (7) the network Euler-Lotka equation (see Section II in SI for an alternative derivation). Although the course of infectiousness and the network topology conspire in determining the spreading rate  $\Lambda$ , these two aspects appear as separated in Eq. (7). Indeed, the right hand side of Eq. (7) only depends on  $\psi(\tau)$  at given  $\Lambda$ , while the left hand side is uniquely determined by the network topology. This latter fact depends on having fixed  $p_\psi = 1$ ; otherwise,  $R$  would have depended on  $p_\psi$  as well (see Section I in SI). Equation (7) predicts that the epidemic threshold, i.e the condition  $\Lambda = 0$ , is obtained by setting  $R = 1$ , independently of  $\psi(\tau)$ .

In general, we shall use Eq. (7) as an implicit relation for the unknown  $\Lambda$ . It is possible to explicitly express  $\Lambda$  from Eq. (7), but only in an approximate way. In particular, using the first two moments of the generation-time distribution, we obtain

$$\Lambda \approx \frac{\ln R}{\langle \tau \rangle} + (\ln R)^2 \frac{\sigma^2}{2\langle \tau \rangle^3}, \quad (8)$$

where  $\sigma^2 = \langle \tau^2 \rangle - \langle \tau \rangle^2$ , see Section II B in SI. An alternative is to combine Eq. (7) with the Jensen inequality, that states that  $\langle e^{-\Lambda \tau} \rangle \geq e^{-\Lambda \langle \tau \rangle}$ . This leads to a lower bound on the exponential spreading rate of the epidemic:

$$\Lambda \geq \frac{\ln R}{\langle \tau \rangle}. \quad (9)$$

The bound in Eq. (9) is saturated when the epidemic spreads at regular time interval, i.e., when  $\psi(\tau)$  is a Dirac delta function.

## Synthetic networks

The network Euler-Lotka equation successfully predicts the rate of epidemic spreading on synthetic complex networks, Fig. 2-a and Fig. 2-b. Our battery of tests includes a broad range of models characterised by different degree distribution, assortativity, and clustering. For each model, we ran simulations using three different infectivity functions, see Fig. 2-c. The choice of the infectivity function qualitatively affect the behaviour of the epidemic. In particular, for peaked distributions, the exponential growth appears modulated by oscillations (Fig. 2-a), since early generations of the epidemic are nearly synchronised. To extrapolate the leading exponential behaviour from these curves, we fit them to a generalised logistic function, which appear to well capture finite-size effects (see Methods). The fits also permits to define a finite-size parameter  $\eta \in [0, 1]$ , which quantifies the relative impact of finite-size effects on the exponential spreading rate at short times (see Methods and Section III in SI). When predicting the exponential growth rate using the network Euler-Lotka equation, we use  $R_{\text{pert}}$  as defined in Eq. (5) as the reproduction number. As expected, the predictions are considerably worse if we instead use  $R_0$ , see Section IV G in SI. The difference between the exponential spreading rate estimated from

the simulations and from the network Euler-Lotka equation (7) is within 6% for all networks, see Fig. 2-c. The only exception is the Barabási-Albert network with parameter  $m = 1$  (average error 15%), where  $m$  represents the number of nodes a new node attaches to.

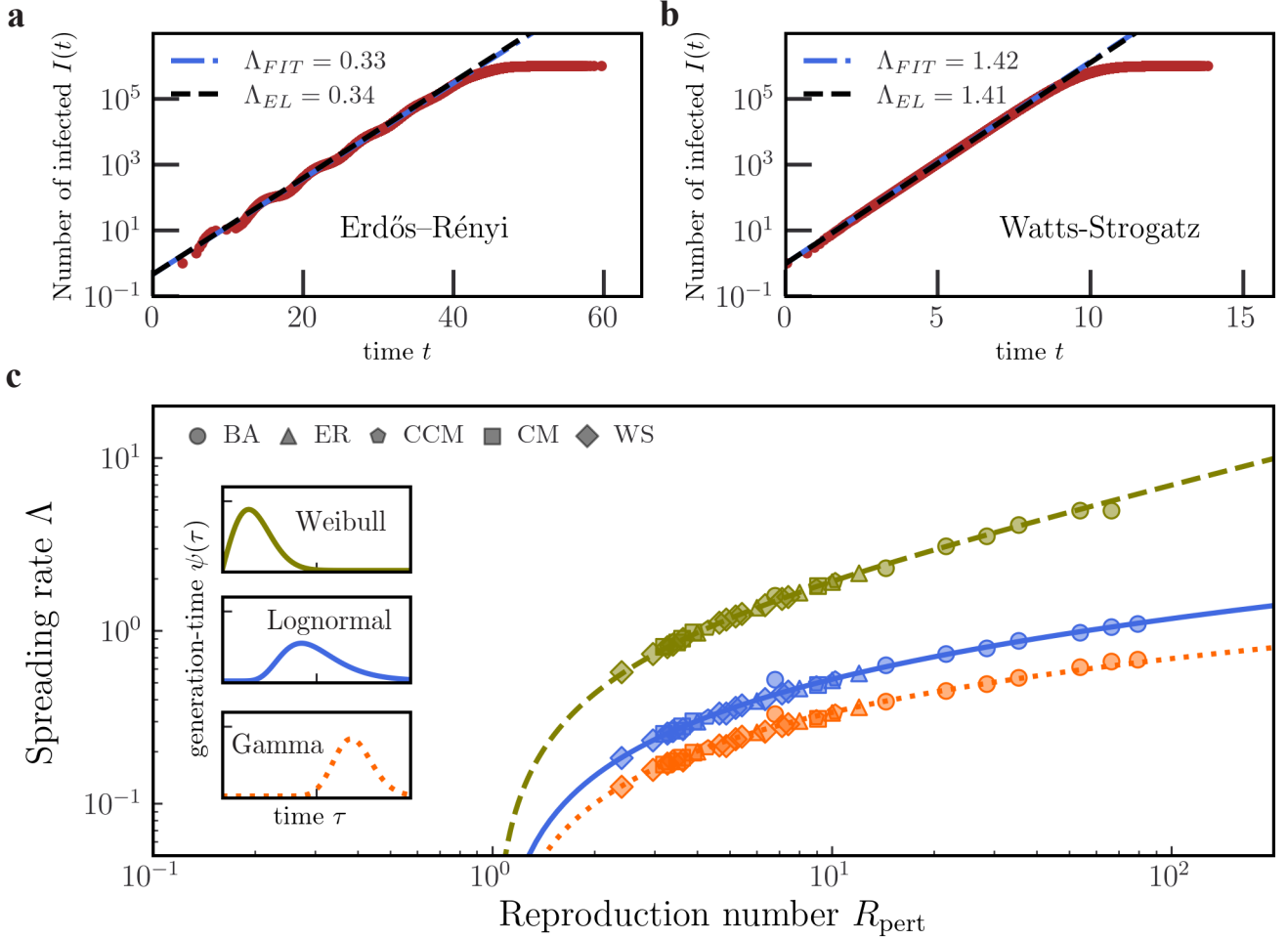


**Figure 2: The network Euler-Lotka equation predicts the rate of epidemic spreading on synthetic networks.:** Panel **a**: Average epidemic on a Erdős-Rényi network of size  $N = 10^6$  with  $\bar{k} = 4$  with Gamma distributed infection times. The red curve is an average over 500 realisations of the epidemic. We estimate the exponential spreading rate (yellow dashed line) by fitting a generalised logistic function on the average trajectory (red dots), see Methods. The black dashed line is the solution of the network Euler-Lotka Equation (7) with  $R = R_{pert}$  as given by Eq. (5). Panel **b**: Same as **a**, but with a Weibull distribution on a Watts-Strogatz network of size  $N = 10^6$ . Panel **c**: Solution of the network Euler-Lotka equation compared with simulations for various networks. The procedure for **a** - **b** is repeated for various networks of sizes  $10^5$  and  $10^6$ : Barabási-Albert (circles); Watts-Strogatz (diamonds); Erdős-Rényi (triangles); networks from the configuration model (CM: squares) with Lognormal and Borel degree distributions; networks from a generalisation of the configuration model (CCM: pentagons) whose assortativity and clustering coefficient have been modified (see Section IV in SI). These simulations are repeated for three generation time distributions: Weibull (dashed green lines), Lognormal (solid blue lines), Gamma (dotted yellow lines). The expressions of these distributions are given in SI Section IV.

There are two causes for this exception. The first is that the exponential regime for this model is not clearly defined, as revealed by the finite-size parameter (see Fig. 2). This issue is likely related with the fact that the second moment  $\bar{k}^2$  of the degree distribution diverges in the infinite size limit. The second cause is that, for  $m = 1$ , the first-order perturbative expansion in  $r$  loses accuracy, as revealed by the difference between  $R_{pert}$  and the leading eigenvalue of the reproductive

matrix (see Table 1).

## Real-world networks

We apply the network Euler-Lotka equation to a large set of social, biological, technological, and transportation networks, see Fig. 3. These real-world networks exhibit more complex structures than synthetic networks. They are often characterised by tightly linked communities, strong degree-correlation and broad tails in the degree distribution. Therefore, they constitute a more challenging test. Nevertheless, the network Euler-Lotka equation holds well, see Fig. 3-a and Fig. 3-b for examples.

More generally, we find that the prediction of the network Euler-Lotka equation well reproduces the fitted spreading rate whenever the finite-size parameter  $\eta$  detects a clear exponential regime, see Fig. 3-c. Although some of these networks are highly clustered, using  $R_{\text{pert}}$  as expressed by Eq. (5) does not perform worse than  $R$  (See Section IV G in SI). In Fig. 3-c, we have omitted three road networks (California, Texas, and Pennsylvania). For these networks, the generalised logistic fit fails to converge. However, a function of the form  $\dot{I}(t) \sim t^\beta$  well fits the epidemic trajectories on these networks (see Section IV D in SI). Likely, the fact that these networks are embedded in a two-dimensional physical space prevents an exponential epidemic spread.

For networks in which our fit detects small finite-size effects ( $\eta < 0.5$ ), the predictions of the network Euler-Lotka equation using  $R_{\text{pert}}$  are more accurate than those using  $R_0$ . However, for larger values of  $\eta$ ,  $R_0$  performs slightly better on average (see Section IV G in SI). Even in these cases,  $R_{\text{pert}}$  provides a better approximation of the reproduction number  $R$ , see SI Fig. 24-b. This suggests that the advantage of  $R_0$  for large  $\eta$  might be due to a compensatory effect: using  $R_0$  tends to overestimate the reproduction number, while the network Euler-Lotka equation tends to underestimate  $\Lambda$  compared to  $\Lambda_{\text{FIT}}$ .

We aim at understanding why, for certain real-world networks, the predicted spreading rate deviates from the fitted one. We find large errors only for scale-free networks in which the finite-size parameter  $\eta$  is also large, see Fig. 4-a. We call a network scale-free if the tail of its degree distribution are fitted by a power law of the form  $k^{-\gamma}$ , with  $\gamma \leq 3$ , multiplied by a slowly varying function, see [28] and Section VI in SI. In contrast, the error is weakly affected by the strength of clustering, see Fig. 4-b. One issue with heavy-tailed networks is that the rapid infection of hubs depletes the tail of the degree distribution of the remaining nodes. This implies that, as the epidemic progresses, the degree distribution of the infected nodes does not remain invariant as assumed by our theory. To test this explanation, we study the average degree  $\bar{k}_n$  of infected individuals in generation  $n$ . In a steady exponential regime, we expect this quantity to be independent of  $n$ , see Fig. 4-c. However, in scale-free networks, the average degree of infected individuals appears to decay as a power-law of their generation, see Fig. 4-d, leading to a non-steady spreading.

## Discussion

In this paper, we developed a theory describing the exponential spreading rate of epidemics in populations arranged on a complex network. Our theory relates the spreading rate to the infectiousness and the social structure, while disentangling the impact of their distinct properties. Our approach accurately predicts the spreading rate on a wide range of model and real networks, aside from networks with heavy-tailed degree distributions where the exponential regime is hindered by finite-size effects.

When analysing the early stage of real epidemics, a departure from an exponential behaviour in the observed number



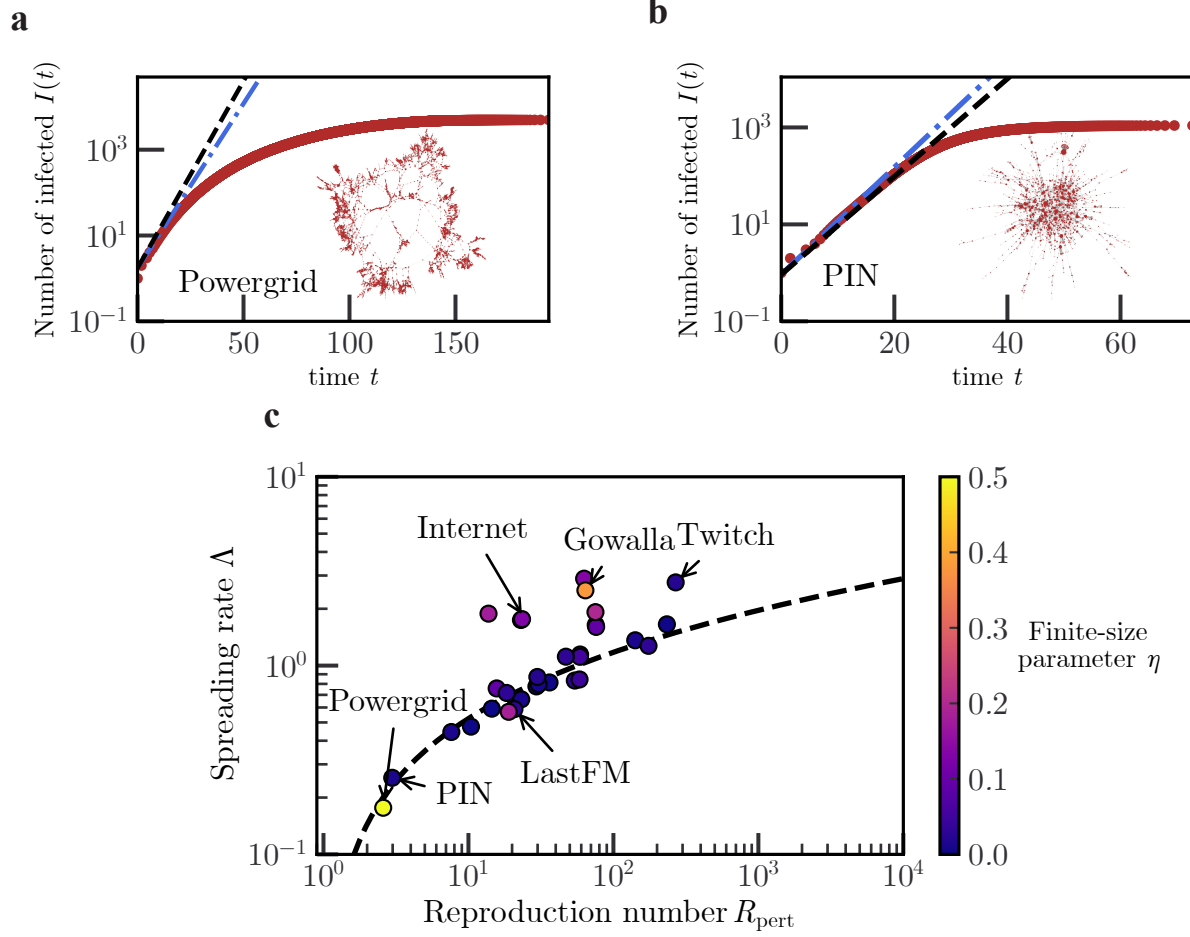


Figure 3: **The network Euler-Lotka equation predicts the epidemic spreading rate on real-world networks.** We simulate epidemic spreading on real-world networks from ICON [25], SNAP [26] and KONECT [27]. All considered networks are undirected and without multiple links or self-connections. Their size varies from  $N = 10^3$  to  $N = 10^6$  (see Section IV B in SI). We simulate 500 epidemics on each of these real-world networks with lognormally distributed infection times, see SI Section IV. Panels **a** and **b** show the average trajectory for two different networks along with a representation of the actual network. Similarly to Figure 2, for each network, we obtain the exponential spreading rate (blue dashed-dotted line) by fitting a generalised logistic function to the average trajectory (red dots). The black dashed line represents the slope predicted by the network Euler-Lotka equation. Panel **c**: Exponential spreading rate for all real-world networks. The solid line is the solution of the Euler-Lotka equation. The markers are the numerical fits. The colour of the marker denotes the value of the finite-size parameter  $\eta$ .

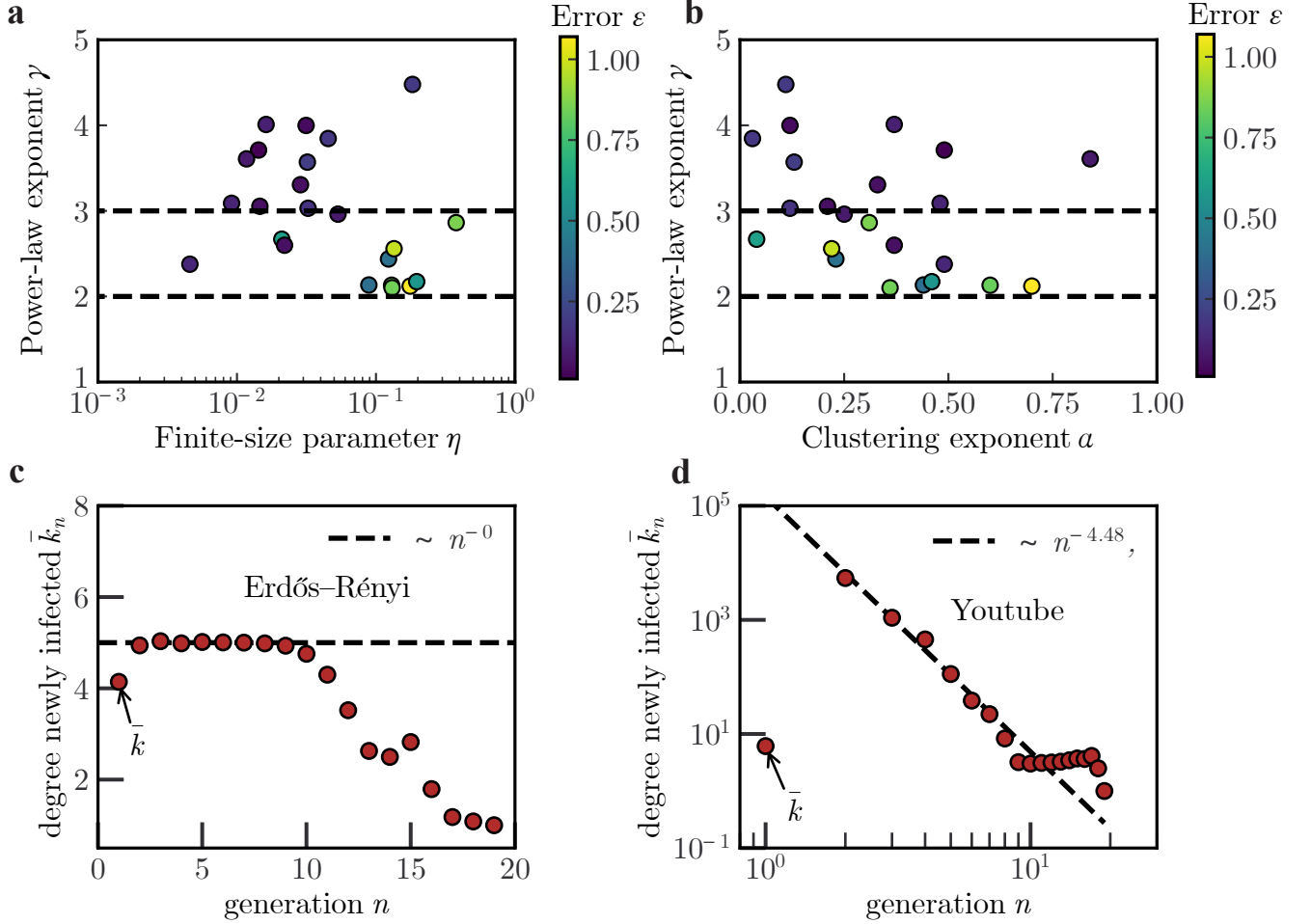


Figure 4: **Finite-size effects impact early stages of an epidemic on scale-free networks**. Panel a: Relative error between the fit and the Euler-Lotka equation as a function of the exponent  $\gamma$  and the finite-size parameter  $\eta$  (see Methods). The error is always low, except when the network is scale-free ( $2 < \gamma \leq 3$ , region between the two dashed lines) and the finite-size parameter  $\eta$  is large. Panel b: Error as a function of  $\gamma$  and the exponent  $\alpha$  of the degree-based clustering coefficient  $c_k \sim (k-1)^{-\alpha}$  which can be interpreted as the strength of the clustering. Panel c: Average degree of individuals infected at the  $n$ th generation on a Erdős-Rényi graph of size  $N = 10^6$  and average degree  $\bar{k} = 4$ . The dashed line is a power-law fit  $\sim n^{-\delta}$  for  $n \in [1, 6]$ . The fit yields  $\delta \approx 0$ , consistently with a steady exponential spreading. Panel d: Average degree of individuals infected at the  $n$ th generation for the Youtube network, which is scale-free ( $\gamma \approx 2.2$  (see Section VI in SI)). The average degree decays as a power law with exponent  $\delta \approx 4.48$  and is therefore not steady.

of cases is often interpreted as a consequence of individual response or early containment measures (see, e.g., [29]). Our results show that non-exponential epidemic trajectories are common in heavy-tailed networks, thus providing an alternative explanation for these observations.

The theory developed in this paper can be also used to estimate the basic reproduction number  $R$  [30]. Ideally, in the early stage of an epidemic, one could use the Euler-Lotka equation to deduce  $R$ . However, this approach is fraught with practical difficulties. First, the curves in Fig. 2f show that a small error in the estimate of the exponential spreading rate  $\Lambda$  can lead to a large uncertainty on  $R$ . Second, it is often difficult to reliably estimate the infectiousness distribution (see, e.g., [31, 32, 33] for the case of COVID-19). Instead, our theory permits to directly estimate  $R$  from structural properties of the interaction networks, such as moments of the degree distribution and clustering. These properties could be inferred,

to some extent, based on contact tracing data [34]. As a consequence, such approach could lead to improved estimates of the infectivity function as well.

We have focused for simplicity on static networks, which is justified when the social structures evolve in a slower way than the time scale of the infection process. If however the time-scales are similar, epidemic dynamics are more complex [35]. For example, bursty social interactions substantially affect epidemic spreading [36]. In principle, interactions could be also weighted, as duration and intensity of contacts affect the probability of transmission [37]. The approach developed in this paper is flexible enough to be extended to these scenarios.

## Methods

### Reproduction Number

We here derive the expression for the reproduction number, Eq. (5). We express the average number of infected individuals at generation  $n \geq 1$  in terms of the reproduction matrix introduced in Eq. (3) by summing over the degree of individuals at each generation:

$$Z_n = \sum_{k_1 \dots k_n} M_{k_n k_{n-1}} M_{k_{n-1} k_{n-2}} \dots M_{k_2 k_1} k_1 P(k_1). \quad (10)$$

At the first generation, we obtain  $Z_1 = \bar{k}$ . For large  $n$ , we have  $Z_n \sim R^n$ , where  $R$  is the leading eigenvalue of  $M_{kk'}$ . For an arbitrary level of clustering and of degree correlation, the leading eigenvalue is not easy to compute exactly. We therefore approximate the eigenvalue by assuming weak clustering and treating the degree correlations as a perturbation of the uncorrelated case.

Degree correlations are summarised by the assortativity  $r$  [38], defined as the Pearson correlation coefficient of the degrees of connected nodes:

$$r = \frac{1}{\sigma_r^2} \sum_{kk'} \left[ kk' P(k, k') - \frac{k^2 k'^2}{\bar{k}^2} P(k) P(k') \right], \quad (11)$$

where  $\sigma_r^2 = \overline{k^3}/\bar{k} - (\overline{k^2}/\bar{k})^2$  ensures that  $-1 \leq r \leq 1$  and  $P(k, k') = k' P(k|k') P(k')/\bar{k}$  is the probability that a randomly chosen edge connects nodes of degrees  $k$  and  $k'$ .

We now analyse the clustering measure  $m_{kk'}$ . While being a measure of clustering,  $m_{kk'}$  also contains information on the degree correlation of connected nodes. In contrast, the degree dependent clustering coefficient  $c_k$  is independent of degree correlations [39]. This coefficient is related to  $m_{kk'}$  as  $(k-1)c_k = \sum_{k'} m_{kk'} P(k'|k)$ . If we assume that  $m_{kk'}$  factorises into  $k$  and  $k'$ -dependent factors, we can express  $m_{kk'}$  as

$$m_{kk'} = \frac{(k-1)c_k (k'-1)c_{k'}}{m_1} \quad (12)$$

where  $m_1 = \overline{k(k-1)c_k}/\bar{k}$ . In particular, this factorisation is justified in the weak clustering limit [39]. Using this expression, we rewrite the reproduction matrix as

$$M_{kk'} = (k'-1) \left[ 1 - c(k') \frac{(k-1)c_k}{m_1} \right] P(k|k') \quad (13)$$

To further simplify the problem, we neglect the dependence on  $k$  of the probability that a node of degree  $k'$  connected to a node of degree  $k$  is part of a triangle. This amounts to assume  $(k-1)c_k/m_1 = 1$ , so that Eq. (13) becomes

$$M_{kk'} = (k'-1)[1 - c(k')]P(k|k'). \quad (14)$$

We now treat  $r$  as a small perturbation parameter and express the leading eigenvalue using perturbation theory. To this aim, we express the reproduction matrix as

$$M_{kk'} = M_{kk'}^{(r=0)} + r\delta M_{kk'}, \quad (15)$$

with

$$M_{kk'}^{(r=0)} = (k' - 1)(1 - c(k')) \frac{k}{\bar{k}} P(k), \quad (16)$$

$$\delta M_{kk'} = (k' - 1)(1 - c(k')) \left( P^{(1)}(k|k') - \frac{k}{\bar{k}} P(k) \right), \quad (17)$$

where we have used that  $P(k|k') = kP(k)/\bar{k}$  for  $r = 0$  and  $P^{(1)}(k|k')$  is unspecified, but satisfies  $\sum_k P^{(1)}(k|k') = 1$  and  $\sum_k kP^{(1)}(k|k') = k'$ . At this order in perturbation theory, the degrees of connected nodes are linearly correlated.

At the first order in  $r$ , we obtain

$$R_{\text{pert}} = (R_0 - m_1)(1 - r) + \frac{r}{R_0 - m_1} \left( \frac{\overline{k(k-1)^2}}{\bar{k}} - 2m_2 + m_1^2 \right) + \mathcal{O}(r^2), \quad (18)$$

see SI, where we defined  $m_2 = \overline{k(k-1)^2 c_k / \bar{k}}$ . At this order, the right eigenvector associated to the unique leading eigenvalue is given by:

$$\begin{aligned} v_k &= \frac{kP(k)}{\bar{k}} + \frac{r}{R_0 - m_1} \sum_{k'} \delta M_{kk'} \frac{k'P(k')}{\bar{k}} \\ &\propto \left[ 1 - r + \frac{r}{R_0 - m_1} ((k-1) - m_1) \right] kP(k). \end{aligned} \quad (19)$$

This eigenvector, if normalised, represents the relative probability that an infected individual has degree  $k$  in the exponential regime.

## Spreading rate of simulated epidemics: Generalised Logistic Function

We describe our extrapolation of the exponential spreading rate  $\Lambda$  of an epidemic from simulation data. In networks with heavy tails, finite-size effects alter the course of the epidemic at relatively early times. Likely for this reason, we have observed that functions such as a simple logistic regression fail to fit well the course of the epidemic. In contrast, we have found that the generalised logistic function

$$I(t) = \frac{N}{(1 + Qe^{-\Lambda_0 \nu t})^{1/\nu}}, \quad (20)$$

well fits the epidemic trajectories for the large majority of networks that we considered. In Eq. (20),  $N$  the size of the network and  $Q = (N/I_0)^\nu - 1$  where  $I_0$  the initial number of infected individuals. Although each simulation starts with a single infected individual, we consider  $I_0$  as a free parameter to better capture the behaviour of the epidemic at the early stages. The remaining free parameters are  $\Lambda_0$  and  $\alpha$ . We fit the logarithm of the generalised logistic function, and discard the first  $\bar{k}$  infection events of each simulation, i.e., the times until  $I(t) = \bar{k}$ . The reason is that these infections should belong to the first generation  $Z_1$ , in which the average number of secondary infections per individual is  $\bar{k}$  rather than  $R$ .

A linearisation of  $\log I(t)$  for small  $t$  in Eq. (20) shows that:

$$\log I(t) = \log I_0 + \Lambda_0 t \left( 1 - \left( \frac{I_0}{N} \right)^\nu \right) + \mathcal{O}(t^2). \quad (21)$$

For  $N \rightarrow \infty$ , we obtain  $I(t) \sim \exp(\Lambda_0 t)$ . Equation (21) leads us to define the finite-size parameter  $\eta = (I_0/N)^\nu$  and the finite-size growth rate  $\Lambda = \Lambda_0(1 - \eta)$ . For  $\nu \rightarrow 1$ , we recover a classic logistic function, while for  $\nu \rightarrow 0$  the generalised

logistic function tends to a Gompertz curve. For the synthetic and real-world networks that we studied, we have found that the finite-size parameter correlates with the curvature of  $\log I(t)$  for small  $t$ , i.e. the deviation from an exponential behaviour (see Section III in SI).

We call  $\Lambda_{\text{FIT}}$  the value of  $\Lambda$  that makes Eq. (20) fit best the data. We call  $\Lambda_{\text{EL}}$  the value of  $\Lambda$  obtained as solution of the Euler-Lotka equation. We measure the quality of our predictions by means of the symmetric relative error:

$$\varepsilon = 2 \frac{|\Lambda_{\text{FIT}} - \Lambda_{\text{EL}}|}{\Lambda_{\text{FIT}} + \Lambda_{\text{EL}}}. \quad (22)$$

The fits of all epidemic trajectories, together with tables presenting all values of the  $\Lambda_{\text{FIT}}$  and  $\Lambda_{\text{EL}}$  are presented in Section IV in SI.

## Acknowledgements

We thank C. Castellano and I. Neri for comments on a preliminary version of this manuscript. We thank Joshua Weitz for discussions. We are grateful for the help and support provided by the Scientific Computing and Data Analysis section of Core Facilities at OIST.

## References

- [1] Buckee, C., Noor, A. & Sattenspiel, L. Thinking clearly about social aspects of infectious disease transmission. *Nature* **595**, 205–213 (2021).
- [2] Patwardhan, S., Rao, V. K., Fortunato, S. & Radicchi, F. Epidemic spreading in group-structured populations. *Physical Review X* **13**, 041054 (2023).
- [3] Granell, C. & Mucha, P. J. Epidemic spreading in localized environments with recurrent mobility patterns. *Physical Review E* **97**, 052302 (2018).
- [4] Kumar, S., Jha, S. & Rai, S. K. Significance of super spreader events in covid-19. *Indian Journal of Public Health* **64**, 139–141 (2020).
- [5] Sneppen, K., Taylor, R. J. & Simonsen, L. Impact of Superspreaders on dissemination and mitigation of COVID-19. *MedRxiv* 2020–05 (2020).
- [6] Newman, M. *Networks* (Oxford university press, 2018).
- [7] Pastor-Satorras, R. & Vespignani, A. Epidemic spreading in scale-free networks. *Physical Review Letters* **86**, 3200 (2001).
- [8] Newman, M. E. Spread of epidemic disease on networks. *Physical Review E* **66**, 016128 (2002).
- [9] Pastor-Satorras, R., Castellano, C., Van Mieghem, P. & Vespignani, A. Epidemic processes in complex networks. *Reviews of Modern Physics* **87**, 925 (2015).
- [10] Barthélemy, M., Barrat, A., Pastor-Satorras, R. & Vespignani, A. Dynamical patterns of epidemic outbreaks in complex heterogeneous networks. *Journal of theoretical biology* **235**, 275–288 (2005).

- [11] Pósfai, M. & Barabási, A.-L. *Network Science* (Citeseer, 2016).
- [12] Ravasz, E. & Barabási, A.-L. Hierarchical organization in complex networks. *Physical Review E* **67**, 026112 (2003).
- [13] Grassly, N. C. & Fraser, C. Mathematical models of infectious disease transmission. *Nature Reviews Microbiology* **6**, 477–487 (2008).
- [14] Weitz, J. S., Park, S. W., Eksin, C. & Dushoff, J. Awareness-driven behavior changes can shift the shape of epidemics away from peaks and toward plateaus, shoulders, and oscillations. *Proceedings of the National Academy of Sciences* **117**, 32764–32771 (2020).
- [15] Barthélemy, M., Barrat, A., Pastor-Satorras, R. & Vespignani, A. Velocity and hierarchical spread of epidemic outbreaks in scale-free networks. *Physical Review Letters* **92**, 178701 (2004).
- [16] Moore, S. & Rogers, T. Predicting the speed of epidemics spreading in networks. *Physical Review Letters* **124**, 068301 (2020).
- [17] Merbis, W. & Lodato, I. Logistic growth on networks: Exact solutions for the susceptible-infected model. *Physical Review E* **105**, 044303 (2022).
- [18] Rose, C. *et al.* Heterogeneity in susceptibility dictates the order of epidemic models. *Journal of Theoretical Biology* **528**, 110839 (2021).
- [19] Berestycki, H., Desjardins, B., Weitz, J. S. & Oury, J.-M. Epidemic modeling with heterogeneity and social diffusion. *Journal of Mathematical Biology* **86**, 60 (2023).
- [20] Hakki, S. *et al.* Onset and window of SARS-CoV-2 infectiousness and temporal correlation with symptom onset: a prospective, longitudinal, community cohort study. *The Lancet Respiratory Medicine* **10**, 1061–1073 (2022).
- [21] Serrano, M. Á. & Boguná, M. Clustering in complex networks. II. Percolation properties. *Physical Review E* **74**, 056115 (2006).
- [22] Callaway, D. S., Newman, M. E., Strogatz, S. H. & Watts, D. J. Network robustness and fragility: Percolation on random graphs. *Physical Review Letters* **85**, 5468 (2000).
- [23] Goltsev, A. V., Dorogovtsev, S. N., Oliveira, J. G. & Mendes, J. F. Localization and spreading of diseases in complex networks. *Physical Review Letters* **109**, 128702 (2012).
- [24] Serrano, M. A. & Boguná, M. Tuning clustering in random networks with arbitrary degree distributions. *Physical Review E* **72**, 036133 (2005).
- [25] Clauset, A., Tucker, E. & Sainz, M. The Colorado Index of Complex Networks. <https://icon.colorado.edu/> (2016).
- [26] Leskovec, J. & Krevl, A. SNAP Datasets: Stanford large network dataset collection. <http://snap.stanford.edu/data> (2014).
- [27] Kunegis, J. KONECT – The Koblenz Network Collection. In *Proc. Int. Conf. on World Wide Web Companion*, 1343–1350 (2013). URL <http://dl.acm.org/citation.cfm?id=2488173>.

- [28] Voitalov, I., Van Der Hoorn, P., Van Der Hofstad, R. & Krioukov, D. Scale-free networks well done. *Physical Review Research* **1**, 033034 (2019).
- [29] Maier, B. F. & Brockmann, D. Effective containment explains subexponential growth in recent confirmed COVID-19 cases in China. *Science* **368**, 742–746 (2020).
- [30] Birello, P., Re Fiorentin, M., Wang, B., Colizza, V. & Valdano, E. Estimates of the reproduction ratio from epidemic surveillance may be biased in spatially structured populations. *Nature Physics* 1–7 (2024).
- [31] Lauer, S. A. *et al.* The incubation period of coronavirus disease 2019 (COVID-19) from publicly reported confirmed cases: estimation and application. *Annals of Internal Medicine* **172**, 577–582 (2020).
- [32] Ferretti, L. *et al.* Quantifying SARS-CoV-2 transmission suggests epidemic control with digital contact tracing. *Science* **368**, eabb6936 (2020).
- [33] Nishiura, H., Linton, N. M. & Akhmetzhanov, A. R. Serial interval of novel coronavirus (COVID-19) infections. *International Journal of Infectious Diseases* **93**, 284–286 (2020).
- [34] Kojaku, S., Hébert-Dufresne, L., Mones, E., Lehmann, S. & Ahn, Y.-Y. The effectiveness of backward contact tracing in networks. *Nature Physics* **17**, 652–658 (2021).
- [35] Cai, C.-R., Nie, Y.-Y. & Holme, P. Epidemic criticality in temporal networks. *Physical Review Research* **6**, L022017 (2024).
- [36] Tkachenko, A. V. *et al.* Stochastic social behavior coupled to COVID-19 dynamics leads to waves, plateaus, and an endemic state. *Elife* **10**, e68341 (2021).
- [37] Ferretti, L. *et al.* Digital measurement of SARS-CoV-2 transmission risk from 7 million contacts. *Nature* **626**, 145–150 (2024).
- [38] Newman, M. E. Assortative mixing in networks. *Physical Review Letters* **89**, 208701 (2002).
- [39] Serrano, M. Á. & Boguna, M. Clustering in complex networks. I. General formalism. *Physical Review E* **74**, 056114 (2006).

# Supplementary information: Rate of Epidemic Spreading on Complex Networks

Samuel Cure, Florian G. Pflug, and Simone Pigolotti

*Biological Complexity Unit, Okinawa Institute of Science and Technology, Onna, Okinawa 904-0495, Japan.*

## CONTENTS

I. Non-normalised generation-time distribution	2
A. Uncorrelated case	2
B. Correlated case	2
II. Large deviation principle	3
A. Equation for the spreading rate	3
B. Gaussian approximation of the spreading rate	5
III. Deviation from the exponential regime	6
IV. Simulations of Epidemics on Networks	6
A. Generating synthetic networks	6
B. Real-world networks	7
C. Simulations	7
D. Power-law fit of the trajectories	8
E. Trajectories Synthetic Networks	10
1. Gamma	10
2. Lognormal	14
3. Weibull	18
F. Trajectories real networks	22
1. Lognormal	22
2. Gamma	25
3. Weibull	28
G. Comparison between estimates of the reproduction number	31
V. Explicit calculation of the reproduction number for networks	31
VI. Estimating the tail of the degree distribution	34
References	36



## I. NON-NORMALISED GENERATION-TIME DISTRIBUTION

In the Main Text, we presented our theory in the case in which the integral  $p_\psi = \int_0^\tau \psi(\tau') d\tau'$ , representing the probability of spreading the infection via a given link, is equal to one. In this section, we extend the theory to the general case where  $0 < p_\psi \leq 1$ .

When  $p_\psi = 1$  the reproduction number  $R$  solely depends on the topology of the network. However, for  $0 < p_\psi < 1$ ,  $R$  also depends on  $p_\psi$ .

In our model, the infection spreads through every link at most once. The case in which the infection fails to spread via a specific link is equivalent to a case in which the link did not exist in the first place. This means that the case  $p_\psi < 1$  can be studied by removing links with uniform probability  $(1 - p_\psi)$ . This procedure alters the degree distribution of the network, which becomes

$$P^{\text{new}}(k) = \sum_q \binom{q}{k} p_\psi^k (1 - p_\psi)^{q-k} P(q). \quad (1)$$

### A. Uncorrelated case

When the network is unassortative and unclustered, the reproduction number scales linearly with  $p_\psi$ :

$$\sum_k (k^2 - k) P^{\text{new}}(k) = p_\psi^2 (\overline{k^2} - \overline{k}) \quad (2)$$

$$\sum_k k P^{\text{new}}(k) = p_\psi \overline{k} \quad (3)$$

$$\implies R_0^{\text{new}} = p_\psi R_0, \quad (4)$$

where  $R_0 = \overline{k^2}/\overline{k} - 1$ . Thus, the epidemic threshold ( $R_0 > 1$ ) is reached when:

$$p_\psi > \frac{\overline{k}}{\overline{k^2} - \overline{k}}. \quad (5)$$

This relation recovers the classic result of epidemic threshold on uncorrelated networks [1, 2].

However, this linear relation does not hold, in general, for clustered or assortative networks. Triangles are vulnerable to link removal since all three links need to remain for a triangle to be preserved. If a given link belongs on average to  $m_1$  triangles, after link removal it belongs on average to only  $m_1 p_\psi^2$  triangles. Therefore, we expect the new reproduction number (in the absence of degree correlations) to scale as:

$$R^{\text{new}(r=0)} = p_\psi R_0 - m_1 p_\psi^2. \quad (6)$$

We test Eq. (6) on a Watts–Strogatz network, which is clustered and has almost no correlation in the connected degrees ( $r \approx 0$ ), see Fig. 1. We observe that Eq. (6) captures well the behaviour of the spreading rate. In conclusion, the effect of link removal reduces the reproduction number while also weakening the effect of clustering. The impact on clustering is not strong enough to observe an increase in the reproduction number as  $p_\psi$  is decreased.

### B. Correlated case

Under node removal with uniform probability  $1 - p_\psi$ , the assortativity  $r$  changes as

$$r^{\text{new}} = r \left( 1 + \frac{p_\psi}{1 - p_\psi} \frac{R_0}{\sigma_r^2} \right)^{-1}, \quad (7)$$

where  $\sigma_r^2 = \overline{k^3}/\overline{k} - (\overline{k^2}/\overline{k})^2$ . Equation (7) is derived in Ref. [3]. Similarly to the derivation in subsection IA, we obtain

$$\frac{\sum_k P^{\text{new}}(k) k(k-1)^2}{\sum_{k'} k' P^{\text{new}}(k')} = p_\psi^2 \frac{\overline{k(k-1)^2}}{\overline{k}} + R_0 p_\psi (1 - p_\psi) \quad (8)$$

and

$$m_2^{\text{new}} \rightarrow p_\psi^3 m_2 + p_\psi^2 (1 - p_\psi) m_1. \quad (9)$$

Therefore, we have

$$R_{\text{pert}}^{\text{new}} = p_\psi (R_0 - m_1 p_\psi) (1 - r^{\text{new}}) + r^{\text{new}} (1 - p_\psi) + \quad (10)$$

$$\frac{r^{\text{new}}}{R_0 - m_1 p_\psi} \left( p_\psi \frac{\overline{k(k-1)^2}}{\overline{k}} - 2p_\psi^2 m_2 - p_\psi m_1 (1 - p_\psi + m_1 p_\psi^2) \right) + \mathcal{O}(r^2), \quad (11)$$

where  $r^{\text{new}}$  is given by Eq. (7). To test Eq. (10), we simulate repeated epidemics with a Gamma generation-time distribution while varying  $p_\psi$  on two different network. First, we consider a synthetic network that is disassortative and exhibit a heavy-tail in its degree distribution, see Fig. 2a. Second, we consider the Amazon network (see Sec. IV B), which presents assortativity, a heavy tail, and clustering. We find that our theory is in good agreements with the simulations, until  $p_\psi$  becomes too small. For small  $p_\psi \approx 0.2$ , the network is too close to the percolation threshold and the generalized logistic fit becomes less reliable.

## II. LARGE DEVIATION PRINCIPLE

### A. Equation for the spreading rate

The network Euler-Lotka equation (Eq. 7 in the Main Text) is derived in the Main Text from the renewal equation (Eq. 6 in the Main Text). Here, we present an alternative derivation which relates the exponential spreading rate  $\Lambda$  to a large deviation principle. This derivation is slightly more lengthy but will permit us to derive an approximate explicit expression for  $\Lambda$ .

In a network of infinite size, we define the exponential spreading rate as

$$\Lambda = \lim_{t \rightarrow \infty} \frac{1}{t} \ln I(t), \quad (12)$$

provided that this limit exists. We first express the number of infected  $I(t)$  in terms of lineages. The epidemic starts with a single infected individual, which we call the root node, and the epidemic progresses as infected individuals

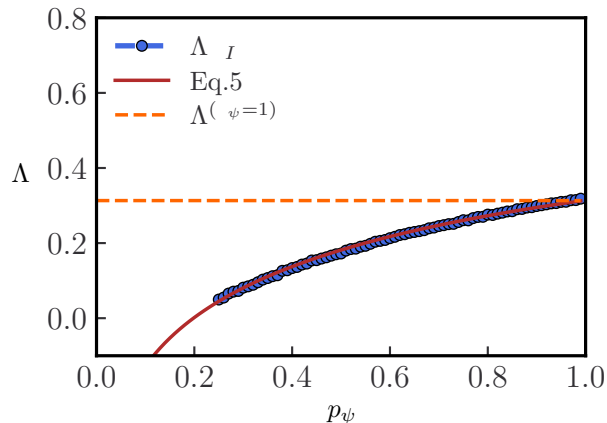


FIG. 1: **Effect of non-normalised generation-time on the spreading rate.** We generate a Watts–Strogatz network with parameter  $k = 6$  and rewiring probability  $p = 0.3$ . We then simulate the average epidemic trajectory over 100 trajectories using a Gamma generation-time distribution (Eq. (32)) but the transmission via a given link only occurs with probability  $p_\psi$ . We repeat this for all  $p_\psi$  and measure the empirical spreading rate (blue markers). We compare it with the spreading rate obtained using Eq. (6) (red line) and include the spreading rate in the case where  $p_\psi = 1$  (orange dashed line).

spread the infection to their neighbours. We call a leaf a node that is infected but has not yet transmitted the disease to any of its neighbours. We define  $L(n, t)$  as the number of leaves at time  $t$  that are at a distance  $n$  from the root. The epidemic passed through  $n$  different nodes before reaching those leaves. The total number of leaves is always smaller or equal to the total number of infected, but grows exponentially at the same rate, so that

$$\Lambda = \lim_{t \rightarrow \infty} \frac{1}{t} \ln \sum_n L(n, t). \quad (13)$$

We express the total number of leaves in the limit  $t \rightarrow \infty$  as

$$\sum_n L(n, t) \approx \sum_n Z_n p_t(n), \quad (14)$$

where  $Z_n$  is the average number of nodes at a distance  $n$  from the root and  $p_t(n)$  is the probability that on a given lineage the infection has spread to a distance  $n$  by time  $t$ . This approximation holds on the assumption that lineages are independent, which is effectively the case for large time. Therefore, we obtain:

$$\Lambda = \lim_{t \rightarrow \infty} \frac{1}{t} \ln \sum_n Z_n p_t(n). \quad (15)$$

This representation allows to separate the properties of the infection times and of the network:  $Z_n$  only depends on the structure of the network while  $p_t(n)$  only depends on  $\psi(\tau)$ . In the case where  $p_\psi = 1$  (see Sec. I), then  $Z_n$  can be interpreted as the number of newly infected at generation  $n$  and scales as  $Z_n \sim R^n$ , where  $R$  is the reproduction number. Therefore, we have:

$$\Lambda = \lim_{t \rightarrow \infty} \frac{1}{t} \ln \langle R^n \rangle_n. \quad (16)$$

where  $\langle \dots \rangle_n$  represents the average over the distribution  $p_t(n)$ . In this representation, the variable  $n$  depends on  $t$  and can be interpreted as a counting process  $n(t)$  with generation-time  $\psi(\tau)$ , such that  $p_t(n)$  is the probability that a lineage is of size  $n$  at time  $t$ .

We now follow the same steps as in Ref. [4]. We define the variable  $\omega = n/t$ , so that  $\omega$  tends to a constant as  $t$  grows large. We say that  $\omega$  satisfies a large deviation principle if

$$p(\omega) \asymp e^{-tI^{(\omega)}(\omega)}, \quad (17)$$

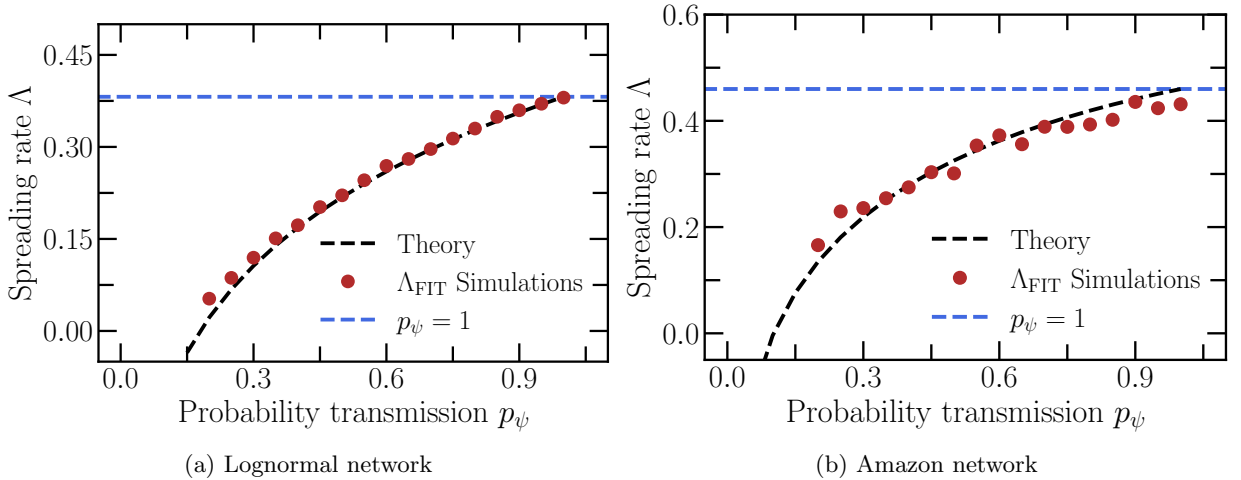


**FIG. 2: Impact of the transmission probability on the epidemic spreading rate.** For each  $p_\psi$  (red markers), we simulate the average epidemic trajectory over 100 trajectories with infection times that are Gamma distributed (Eq. (32)). We run the simulations on a network whose degree are lognormally distributed (Eq. (33)), Panel (a). We repeat this for the Amazon network, Panel (b). The black dashed line represent the solution of the Euler-Lotka equation when we use  $R_{\text{pert}}$  from Eq. (10).

where  $I^{(\omega)}(\omega)$  is called the rate function and where the sign  $\asymp$  means that as  $t \rightarrow \infty$  the dominant part of  $p(\omega)$  is the decaying exponential  $e^{-tI^{(\omega)}(\omega)}$ . Assuming that  $\omega$  satisfies a large deviation principle and that the rate function is convex, we apply the Gärtner-Ellis theorem

$$\Psi^{(\omega)}(q) = \sup_{\omega} \left[ q\omega - I^{(\omega)}(\omega) \right], \quad (18)$$

where  $\Psi^{(\omega)}(q) = \lim_{t \rightarrow \infty} t^{-1} \ln \langle e^{qt\omega} \rangle_{\omega}$  is the scaled cumulant generating function of  $\omega$ . Using in succession Eq. (16) and Eq. (18) we obtain

$$\Lambda = \sup_{\omega} \left[ \omega \ln R - I^{(\omega)}(\omega) \right]. \quad (19)$$

To determine  $I^{(\omega)}(\omega)$  we remember that  $n(t)$  is described by a renewal process with generation-time  $\psi(\tau)$ . This means that its inverse  $t(n)$  is the sum of  $n$  I.I.D random variables distributed according to  $\psi(\tau)$ . Following Ref. [5], their rate functions are related by

$$I^{(\omega)}(x) = xI^{(t)}(1/x). \quad (20)$$

The scaled cumulant generating function of  $t$  can be expressed in terms of the probability density distribution of the infection times:

$$\Psi^{(t)}(q) = \lim_{n \rightarrow \infty} \frac{1}{n} \ln \left\langle e^{q \sum_{i=1}^n \tau_i} \right\rangle_{\tau} = \lim_{n \rightarrow \infty} \frac{1}{n} \ln \prod_{i=1}^n \langle e^{q\tau_i} \rangle_{\tau} = \ln \langle e^{q\tau} \rangle_{\tau}. \quad (21)$$

Applying once again the Gärtner-Ellis theorem, we find

$$I^{(t)}(1/x) = \sup_q \left[ \frac{q}{x} - \ln \langle e^{q\tau} \rangle_{\tau} \right]. \quad (22)$$

Combining this result with Eq. (20), we obtain

$$I^{(\omega)}(x) = x \sup_q \left[ \frac{q}{x} - \ln \langle e^{q\tau} \rangle_{\tau} \right]. \quad (23)$$

Substituting this in Eq. (19), we find

$$\Lambda = \sup_{\omega} \inf_q \left[ \omega \ln R - q + \omega \ln \langle e^{q\tau} \rangle_{\tau} \right] \quad (24)$$

The extremality condition with respect to  $\omega$  is expressed by

$$\langle e^{q\tau} \rangle_{\tau} = \frac{1}{R} \quad (25)$$

Substituting it back in Eq. (24), we obtain  $\Lambda = -q^{\text{inf}}$ . Inserting this in the extremality condition gives the Euler-Lotka equation, Eq. (7) in the Main Text.

## B. Gaussian approximation of the spreading rate

In this section, we derive the approximate expression for  $\Lambda$ , Eq. (8) in the Main Text. In the limit  $t \rightarrow \infty$ , the distribution of the counting process  $n(t)$  tends to a Gaussian with mean  $\mu_n = t/\bar{\tau}$  and variance  $\sigma_n^2 = t\sigma^2/\bar{\tau}^3$  where  $\sigma^2 = \bar{\tau}^2 - \bar{\tau}^2$  is the variance of the generation-time distribution  $\psi(\tau)$ . Using Eq. (16), we thus represent  $\Lambda$  as an average over a Gaussian distribution:

$$\Lambda = \lim_{t \rightarrow \infty} \frac{1}{t} \ln \langle e^{n \ln R} \rangle_n \quad (26)$$

$$\approx \lim_{t \rightarrow \infty} \frac{1}{t} \ln \int_{-\infty}^{+\infty} e^{-\frac{(n-\mu_n)^2}{2\sigma_n^2} + n \ln R} dn \quad (27)$$

$$= \lim_{t \rightarrow \infty} \frac{1}{t} \ln \left( e^{\mu_n \ln R + ((\ln R)^2 \sigma_n^2)/2} \right) \quad (28)$$

$$= \frac{\ln R}{\langle \tau \rangle} + (\ln R)^2 \frac{\sigma^2}{2 \langle \tau \rangle^3}. \quad (29)$$

This formula illustrates how a larger variance contributes to a faster spreading epidemic, while a larger mean tends to slow down the spreading rate.

### III. DEVIATION FROM THE EXPONENTIAL REGIME

If the epidemic spreading were purely exponential, then  $\ell(t) = \ln I(t)$  should appear as a perfectly linear function of  $t$ . To quantify the deviation from the exponential regime, we therefore consider the curvature  $\kappa$  of  $\ell(t)$ :

$$\kappa = \frac{\ell''(t)}{\left(1 + (\ell'(t))^2\right)^{3/2}}. \quad (30)$$

A large curvature indicates a marked deviation from exponential growth. To compare epidemic trajectories between networks, we compute the curvature as given by the generalized logistic equation for  $t = 0$ :

$$\kappa = \frac{\Lambda^2 \nu N^\nu (N^\nu - 1)}{(\Lambda^2 + (\Lambda^2 + 1) N^{2\nu} - 2\Lambda^2 N n^\nu)^{3/2}} + \mathcal{O}(t), \quad (31)$$

where we have set  $I_0 = 1$  to lighten the formula. We plot Eq. (31) as a function of  $\eta$  for various networks, see Fig. 3. We observe a strong log-log positive correlation between the curvature  $\kappa$  and the finite-size parameter  $\eta$ , supporting that the finite-size parameter can be taken as a proxy for the deviation from an exponential behaviour.

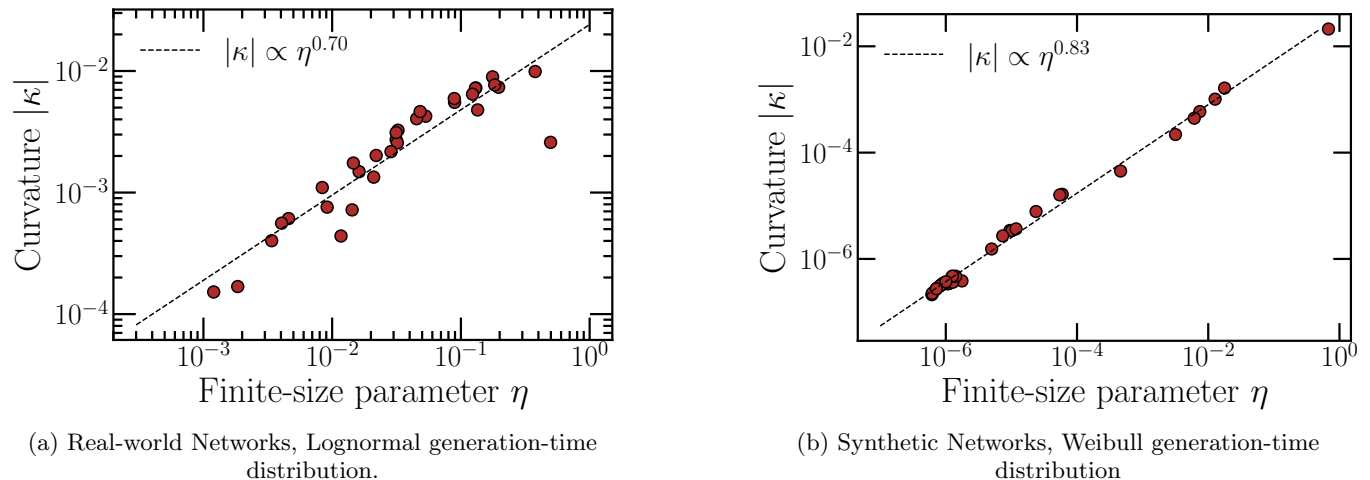


FIG. 3: **Relationship between curvature and finite-size parameter.** For each epidemic trajectory, (a) real-world networks, (b) synthetic networks, we determine the parameters that best fit the generalised logistic function and compute  $\eta$  and  $\kappa$ . The Pearson correlation coefficient between  $\ln(\kappa)$  and  $\ln(\eta)$  is 0.92 in (a) and 0.99 in (b).

### IV. SIMULATIONS OF EPIDEMICS ON NETWORKS

#### A. Generating synthetic networks

We generate Erdős-Rényi, Barabási-Albert, and Watts-Strogatz networks using standard algorithms [6]. We also generate networks with arbitrary degree distribution by means of the configuration model [6] which consists in assigning to every node a number of stubs (half-links) according to a given degree sequence. Then each pair of stub is randomly chosen and connected via a link. Self-links and multiple links can appear, but their number is of the order  $\mathcal{O}(\infty/N)$ , where  $N$  is the number of nodes in the network. In the limit of large  $N$ , the network possesses a tree-like structure (no short loops) and the degrees of connected nodes are uncorrelated ( $r \approx 0$ ).

We tune the assortativity in a given network as follows. We choose two pairs of connected nodes  $a, b, c, d$ , arranged such that  $k_a \leq k_b \leq k_c \leq k_d$ . We rewire the links by forming new pairs  $a - b$  and  $c - d$  to increase assortativity, or  $a - d$  and  $b - c$  to decrease assortativity. This operation preserves the degree distribution while inducing degree correlation.

To generate networks with a tunable clustering coefficient, we implement an algorithm that generalises the configuration model [7]. In our implementation, we start with a degree sequence generated from a distribution  $P(k)$  and

choose an exponent  $\alpha$  so that the number of triangles being part of a node of degree  $k$  is on average  $(k-1)c_k$ , so that  $c_k = a(k-1)^{-\alpha}$ . See Ref. [7] for more details.

TABLE I: Comparison of the properties of all considered synthetic networks.

Network	$N$	$r$	$\bar{c}$	$m_1$	$\bar{k}$	$R_0$	$R$	$R_{\text{pert}}$	Error
BA <sub>1</sub>	$1.0 \times 10^6$	-0.010	0.0	0.0	2.0	13.9	8.5	6.8	0.21
BA <sub>2</sub>	$1.0 \times 10^6$	-0.008	$1.2 \times 10^{-4}$	0.1	4.0	20.4	15.5	14.4	0.07
BA <sub>3</sub>	$1.0 \times 10^6$	-0.008	$1.3 \times 10^{-4}$	0.2	6.0	27.8	22.6	21.6	0.04
BA <sub>4</sub>	$1.0 \times 10^6$	-0.007	$1.4 \times 10^{-4}$	0.3	8.0	34.5	29.4	28.6	0.03
BA <sub>5</sub>	$1.0 \times 10^6$	-0.006	$1.8 \times 10^{-4}$	0.0	10.0	41.0	35.9	35.5	0.01
BA <sub>8</sub>	$1.0 \times 10^6$	-0.005	$2.2 \times 10^{-4}$	0.7	16.0	58.6	54.5	53.7	0.01
BA <sub>10</sub>	$1.0 \times 10^6$	-0.004	$2.6 \times 10^{-4}$	1.3	20.0	72.1	67.7	66.5	0.02
BA <sub>12</sub>	$1.0 \times 10^6$	0.004	$3.0 \times 10^{-4}$	1.8	24.0	85.4	80.8	79.5	0.02
ER <sub>4</sub>	$1.0 \times 10^6$	0.0	0.0	0.0	4.0	4.0	4.0	4.0	0.0
ER <sub>6</sub>	$1.0 \times 10^6$	0.0	0.0	0.0	6.0	6.0	6.0	6.0	0.0
ER <sub>8</sub>	$1.0 \times 10^6$	0.0	0.0	0.0	8.0	8.0	8.0	8.0	0.0
ER <sub>10</sub>	$1.0 \times 10^6$	-0.0	0.0	0.0	10.0	10.0	10.0	10.0	0.0
ER <sub>12</sub>	$1.0 \times 10^6$	0.0	0.0	0.0	12.0	12.0	12.0	12.0	0.0
ER <sub>10</sub> $\alpha = 0.2$	$1 \times 10^5$	0.06	0.1	1.0	10.0	10.0	9.0	9.1	0.01
ER <sub>4</sub> $\alpha = 2$	$1 \times 10^5$	0.04	0.1	0.2	4.1	4.0	4.0	3.9	0.02
ER <sub>4</sub> $\alpha = 0.5$	$1 \times 10^5$	0.04	0.2	0.6	4.1	4.0	3.4	3.5	0.02
LN <sub>4,1</sub> $\alpha = 0.5$	$1.0 \times 10^5$	0.01	0.2	0.6	4.5	3.7	3.2	3.2	0.01
LN <sub>4,1</sub> $\alpha = 2$	$1.0 \times 10^5$	0.02	0.1	0.1	4.5	3.7	3.6	3.6	0.0
LN <sub>10,12</sub>	$1.0 \times 10^6$	-0.0	0.0	0.0	10.0	10.2	10.2	10.2	0.0
LN <sub>4,1</sub>	$1.0 \times 10^6$	-0.0	0.0	0.0	4.0	3.3	3.3	3.3	0.0
BT <sub>2,4</sub>	$1.0 \times 10^5$	0.0	0.0	0.0	5.0	4.3	4.3	4.3	0.0
BT <sub>5,4</sub>	$1.0 \times 10^5$	-0.0	0.0	0.0	8.0	9.0	9.0	9.0	0.01
WS <sub>4,2</sub>	$1.0 \times 10^6$	-0.04	0.3	0.8	4.0	3.2	2.4	2.4	0.0
WS <sub>4,6</sub>	$1.0 \times 10^6$	-0.1	0.0	0.1	4.0	3.4	3.3	3.3	0.0
WS <sub>4,8</sub>	$1.0 \times 10^6$	-0.11	0.0	0.0	4.0	3.5	3.4	3.4	0.0
WS <sub>6,2</sub>	$1.0 \times 10^6$	-0.03	0.3	1.5	6.0	5.2	3.6	3.6	0.0
WS <sub>6,4</sub>	$1.0 \times 10^6$	-0.05	0.1	0.7	6.0	5.3	4.6	4.6	0.0
WS <sub>6,6</sub>	$1.0 \times 10^6$	-0.07	0.0	0.2	6.0	5.4	5.2	5.2	0.0
WS <sub>6,8</sub>	$1.0 \times 10^6$	-0.07	0.0	0.0	6.0	5.5	5.4	5.4	0.0
WS <sub>8,2</sub>	$1.0 \times 10^6$	-0.02	0.3	2.3	8.0	7.2	4.9	4.9	0.0
WS <sub>8,4</sub>	$1.0 \times 10^6$	-0.04	0.1	1.0	8.0	7.3	6.3	6.3	0.0
WS <sub>8,6</sub>	$1.0 \times 10^6$	-0.05	0.0	0.3	8.0	7.4	7.1	7.1	0.0
WS <sub>8,8</sub>	$1.0 \times 10^6$	-0.06	0.0	0.0	8.0	7.5	7.4	7.4	0.0

## B. Real-world networks

We collected real networks available from various databases: SNAP [8], ICON [9] and KONECT [10]. We selected networks of size  $N > 1000$ , only possessing undirected links, not temporal, and not bipartite. The properties of the selected networks and their estimated reproduction number are listed in Table II.

## C. Simulations

We simulate the average trajectory of an epidemic over 500 trajectories for every network. We repeat the simulations for three different infection time distributions: a Gamma distribution with mean 7 and variance 1:

$$\psi_{\text{gam}}(\tau) = \frac{e^{-\frac{m\tau}{v}} \left(\frac{v}{m\tau}\right)^{-\frac{m^2}{v}}}{\tau \Gamma\left(\frac{m^2}{v}\right)}, \quad m = 7, v = 1; \quad (32)$$

TABLE II: Comparison of the properties of all the considered real-world networks.

Network	$N$	$r$	$\bar{c}$	$m_1$	$\bar{k}$	$R_0$	$R$	$R_{\text{pert}}$	Error
amazon	$2.6 \times 10^5$	-0.0	0.4	2.4	6.9	10.1	7.9	7.6	0.03
asCaida	$2.6 \times 10^4$	-0.19	0.2	2.0	4.0	279.2	43.6	23.0	0.47
asOregon	$1.1 \times 10^4$	-0.19	0.3	2.3	4.1	251.2	31.3	13.8	0.56
astroPh	$1.9 \times 10^4$	0.21	0.6	20.5	21.1	64.4	52.5	58.9	0.12
brightkite	$5.8 \times 10^4$	0.01	0.2	6.9	7.4	62.7	53.4	58.8	0.1
condMat	$2.3 \times 10^4$	0.14	0.6	5.6	8.1	21.1	19.7	21.4	0.09
DBLP	$3.2 \times 10^5$	0.27	0.6	6.4	6.6	20.7	18.3	23.1	0.26
deezerEurope	$2.8 \times 10^4$	0.1	0.1	1.5	6.6	15.2	15.5	15.7	0.01
deezerHR	$5.5 \times 10^4$	0.2	0.1	4.0	18.3	34.9	36.1	36.2	0.01
deezerHU	$4.8 \times 10^4$	0.21	0.1	1.3	9.4	14.2	14.6	14.5	0.01
deezerRO	$4.2 \times 10^4$	0.11	0.1	0.8	6.0	10.1	10.3	10.4	0.01
douban	$1.5 \times 10^5$	-0.18	0.0	0.4	4.2	35.9	32.0	29.4	0.08
email	$3.7 \times 10^4$	-0.11	0.5	11.9	10.0	139.1	83.5	76.0	0.09
fbArtist	$5.1 \times 10^4$	-0.02	0.1	8.3	32.4	155.7	142.4	141.4	0.01
fbAthletes	$1.4 \times 10^4$	-0.03	0.3	4.9	12.5	37.4	30.5	30.5	0.0
fbCompany	$1.4 \times 10^4$	0.01	0.2	3.3	7.4	21.0	18.1	18.4	0.02
fbNewSites	$2.8 \times 10^4$	0.02	0.3	5.7	14.8	49.5	47.4	47.0	0.01
fbPublicFigures	$1.2 \times 10^4$	0.2	0.2	8.3	11.6	49.6	51.6	54.2	0.05
github	$3.8 \times 10^4$	-0.08	0.2	5.4	15.3	440.0	106.9	62.8	0.41
gowalla	$2.0 \times 10^5$	-0.03	0.2	7.2	9.7	305.6	115.2	64.1	0.44
hamsterster	$9.2 \times 10^2$	-0.12	0.2	4.3	8.8	32.9	22.2	24.2	0.09
internet	$2.3 \times 10^4$	-0.2	0.2	2.9	4.2	260.5	44.8	23.4	0.48
lastfm	$7.6 \times 10^3$	0.02	0.2	4.4	7.3	24.4	17.7	20.8	0.17
livemocha	$1.0 \times 10^5$	-0.15	0.1	4.6	42.1	326.6	251.2	233.8	0.07
museaFacebook	$2.2 \times 10^4$	0.09	0.4	14.0	15.2	60.1	50.2	58.4	0.16
pgp	$1.1 \times 10^4$	0.24	0.3	6.8	4.6	17.9	12.9	19.0	0.47
PIN	$1.9 \times 10^3$	-0.16	0.1	0.7	2.4	5.5	3.8	3.0	0.22
powergrid	$4.9 \times 10^3$	0.0	0.1	0.3	2.7	2.9	2.5	2.6	0.02
roadCA	$2.0 \times 10^6$	0.13	0.0	0.1	2.8	2.2	2.1	2.1	0.02
roadPA	$1.1 \times 10^6$	0.12	0.0	0.1	2.8	2.2	2.1	2.1	0.0
roadTX	$1.4 \times 10^6$	0.13	0.0	0.1	2.8	2.1	2.1	2.1	0.03
wordnet	$1.5 \times 10^5$	-0.06	0.6	5.2	9.0	54.6	37.8	29.9	0.21

a Log-normal distribution with mean 5 and variance 3:

$$\psi_{\log}(\tau) = \frac{\exp\left(-\frac{\left(\log(t) - \log\left(\frac{m^2}{\sqrt{m^2+v}}\right)\right)^2}{2 \log\left(\frac{v}{m^2} + 1\right)}\right)}{\sqrt{2\pi t} \sqrt{\log\left(\frac{v}{m^2} + 1\right)}}, \quad m = 5, v = 3; \quad (33)$$

and a Weibull distribution with scale 2 and shape 2:

$$\psi_{\text{wei}}(\tau) = \frac{1}{2} e^{-\frac{\tau^2}{4}} \tau. \quad (34)$$

The epidemic starts with one infected individual, chosen uniformly at random. To simulate the epidemics, we implemented a next reaction scheme [11].

#### D. Power-law fit of the trajectories

The fitting procedure of a generalised logistic function described in Methods fails for epidemics on the California, Pennsylvania, and Texas road networks [8]. Instead, their behaviour appears more similar to a power-law  $I(t) \propto t^\beta$ . We therefore fit a power-law to three US road networks, the US powergrid, and compare it to the Condensed Matter citation network, that has a clear exponential phase, see Fig. 4. The power-law fits are excellent for the US road networks, while the generalised logistic function provides a better fit for the US powergrid network. This supports

that finite-size effects ( $\eta = 0.497$ ) are more likely to explain the deviation from the predicted spreading rate for the powergrid network ( $\Lambda_{\text{EL}} = 0.196$  versus  $\Lambda_{\text{FIT}} = 0.351$ ) rather than the presence of a power-law behaviour.

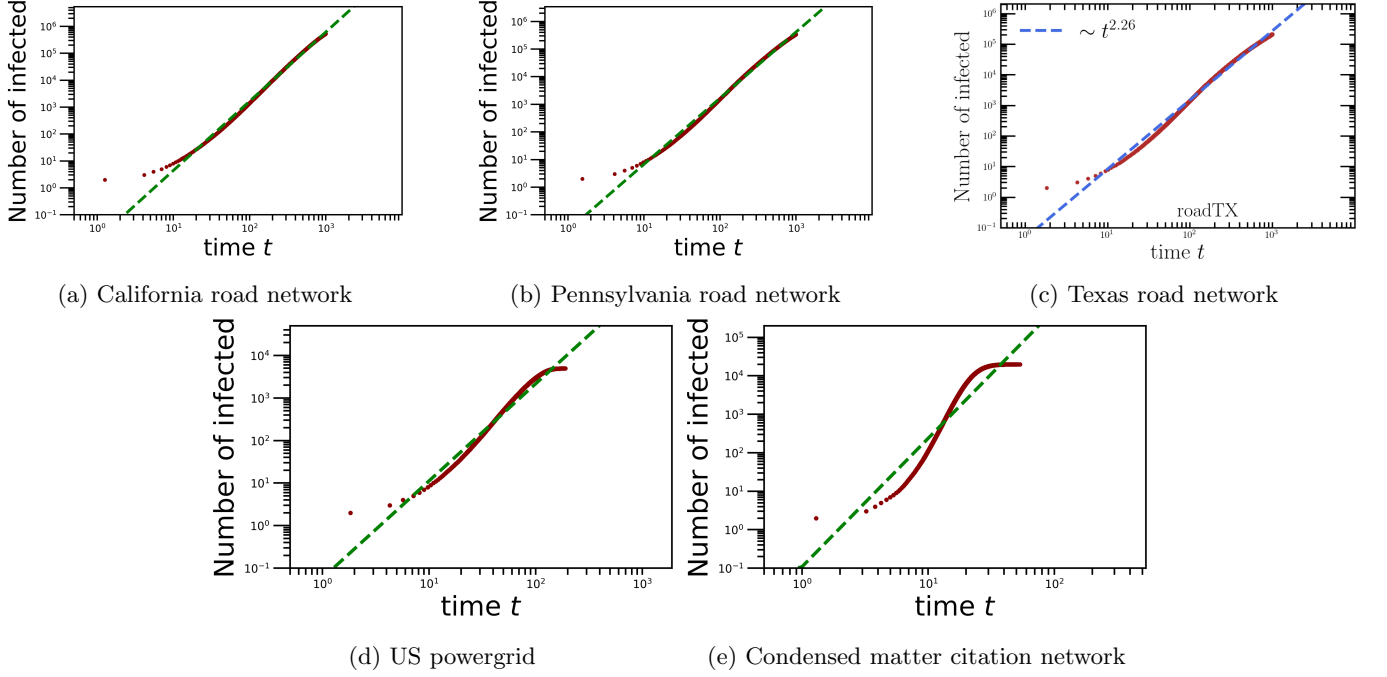


**FIG. 4: Comparison between power-law fit and generalised logistic fit for road networks.** We plot the average epidemic trajectories (red dots) for the three road networks (panels (a)-(b)-(c)), the US powergrid (d) and the condensed matter citation network (e). We fit a power-law (blue) and the generalised logistic function (black) for each trajectory. The infection times are lognormally distributed, see Eq. (32).



## E. Trajectories Synthetic Networks

### 1. Gamma

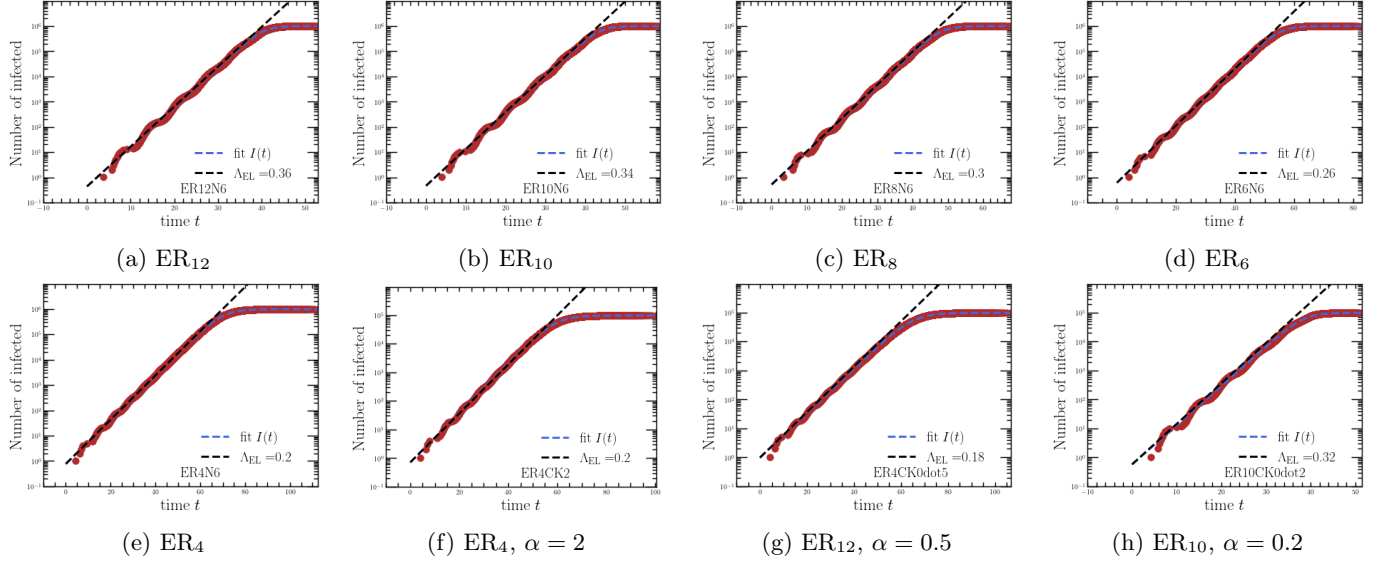


FIG. 5: Average epidemic trajectories on Erdős-Rényi networks with a Lognormal generation-time distribution.

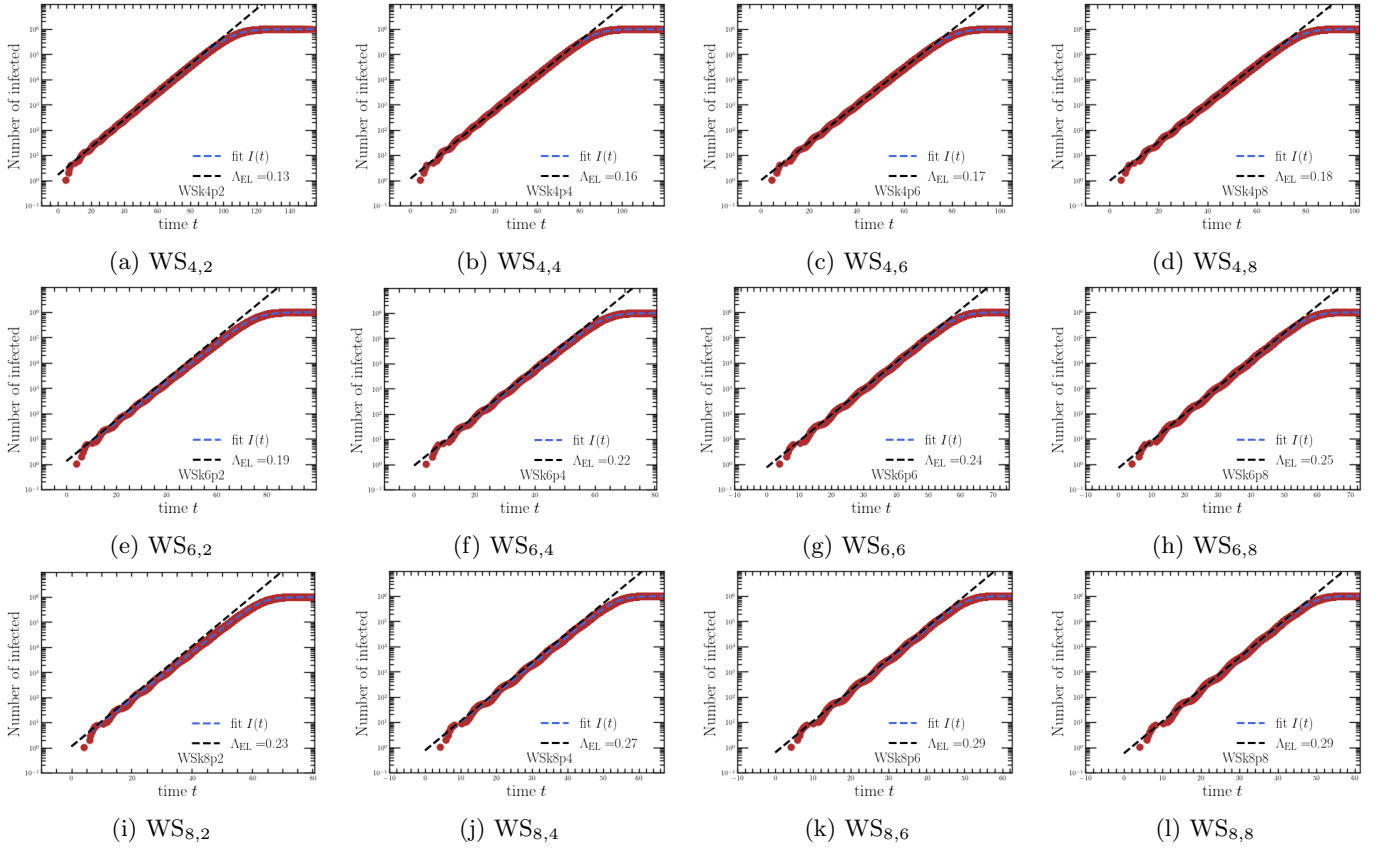


FIG. 6: Average epidemic trajectories on Watts–Strogatz networks with a Lognormal generation-time distribution.

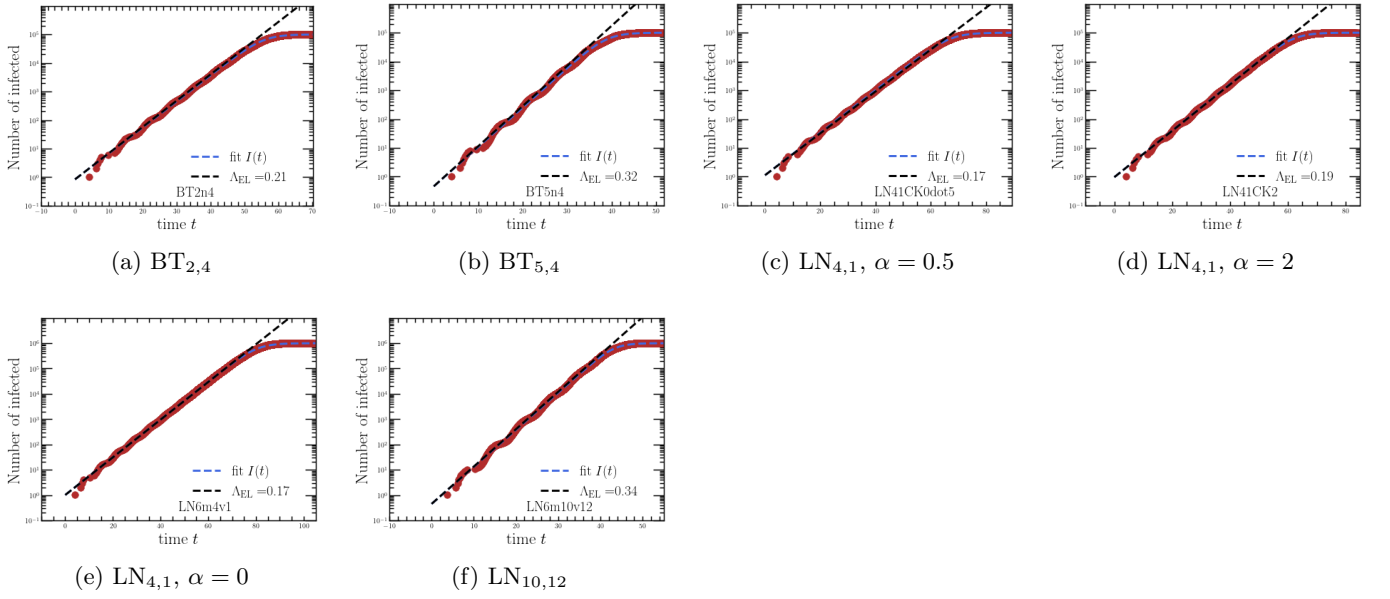


FIG. 7: Average epidemic trajectories on networks from the configuration model with a Gamma generation-time distribution.

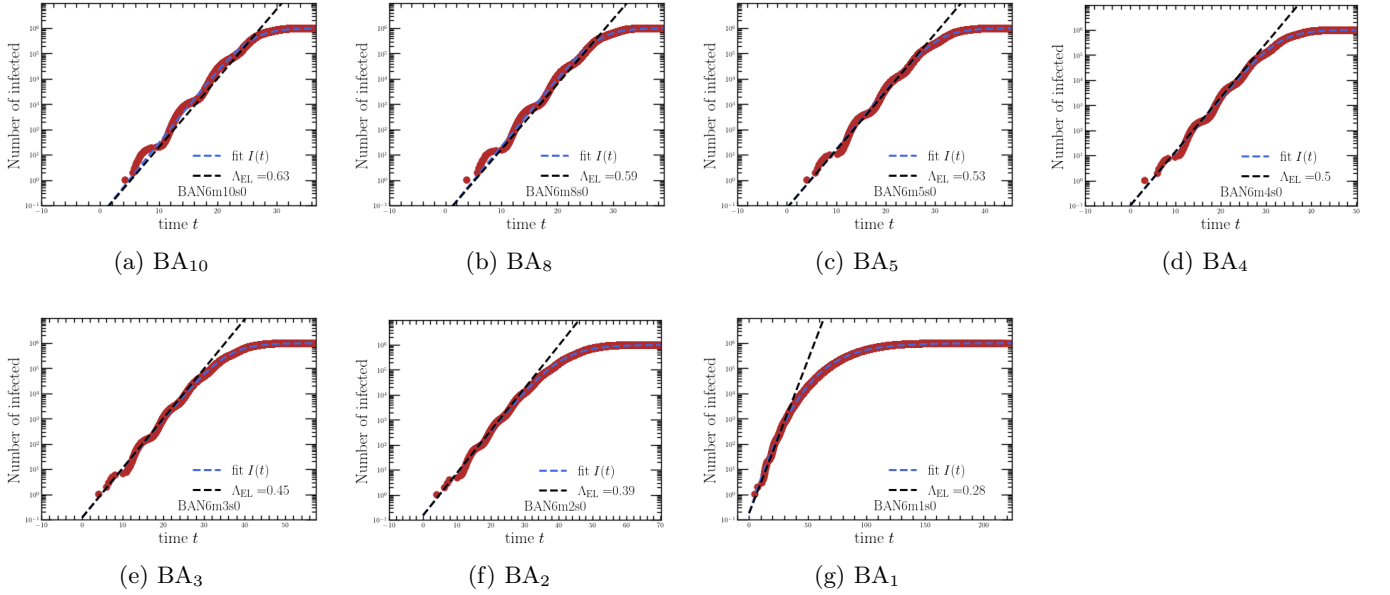


FIG. 8: Average epidemic trajectories on Barabási-Albert networks with a Gamma generation-time distribution.

TABLE III: Results of the fitting procedure for synthetic networks with a Gamma generation-time distribution

Network	$\Lambda_{\text{FIT}}$	$\Lambda_R$	Error $_R$	$\Lambda_{R_{\text{pert}}}$	Error $_{R_{\text{pert}}}$	$\Lambda_{R_0}$	Error $_{R_0}$	$\Lambda_0$	$I_{0(\text{fit})}$	$\nu$
BA <sub>1</sub>	0.33	0.31	-0.05	0.28	-0.17	0.39	0.16	0.44	0.18	0.09
BA <sub>2</sub>	0.39	0.4	0.03	0.39	0.0	0.44	0.13	0.39	0.15	0.45
BA <sub>3</sub>	0.45	0.46	0.02	0.45	0.01	0.49	0.09	0.45	0.12	0.55
BA <sub>4</sub>	0.49	0.5	0.02	0.5	0.01	0.52	0.07	0.49	0.1	0.61
BA <sub>5</sub>	0.54	0.53	-0.01	0.53	-0.02	0.55	0.03	0.54	0.08	0.62
BA <sub>8</sub>	0.62	0.6	-0.04	0.59	-0.05	0.61	-0.02	0.62	0.04	0.65
BA <sub>10</sub>	0.67	0.63	-0.06	0.63	-0.06	0.64	-0.04	0.67	0.04	0.62
BA <sub>12</sub>	0.68	0.66	-0.04	0.65	-0.05	0.67	-0.03	0.68	0.04	0.68
ER <sub>4</sub>	0.2	0.2	0.0	0.2	0.0	0.2	0.0	0.2	0.77	1.12
ER <sub>6</sub>	0.26	0.26	0.01	0.26	0.01	0.26	0.01	0.26	0.61	1.28
ER <sub>8</sub>	0.3	0.3	0.01	0.3	0.01	0.3	0.01	0.3	0.52	1.37
ER <sub>10</sub>	0.33	0.34	0.01	0.34	0.01	0.34	0.01	0.33	0.46	1.42
ER <sub>12</sub>	0.36	0.36	0.01	0.36	0.01	0.36	0.01	0.36	0.43	1.47
ER <sub>10</sub> $\alpha = 0.2$	0.31	0.32	0.03	0.32	0.03	0.34	0.08	0.31	0.57	1.47
ER <sub>4</sub> $\alpha = 2$	0.2	0.2	0.0	0.2	-0.01	0.2	0.01	0.2	0.71	1.09
ER <sub>4</sub> $\alpha = 0.5$	0.18	0.18	0.01	0.18	0.02	0.2	0.13	0.18	0.98	1.1
LN <sub>4,1</sub> $\alpha = 0.5$	0.17	0.17	-0.02	0.17	-0.01	0.19	0.12	0.17	1.13	1.42
LN <sub>4,1</sub> $\alpha = 2$	0.19	0.19	-0.0	0.19	-0.0	0.19	0.03	0.19	0.96	1.44
BT <sub>2,4</sub>	0.21	0.21	0.01	0.21	0.01	0.21	0.01	0.21	0.84	1.48
BT <sub>5,4</sub>	0.32	0.32	0.02	0.32	0.02	0.32	0.02	0.32	0.46	1.3
LN <sub>10,12</sub>	0.34	0.34	0.01	0.34	0.01	0.34	0.01	0.34	0.45	1.41
LN <sub>4,1</sub>	0.17	0.17	-0.0	0.17	-0.0	0.17	-0.0	0.17	1.01	1.35
WS <sub>4,2</sub>	0.13	0.13	0.01	0.13	0.01	0.17	0.29	0.13	1.65	1.23
WS <sub>4,4</sub>	0.16	0.16	-0.0	0.16	-0.0	0.17	0.1	0.16	1.17	1.31
WS <sub>4,6</sub>	0.17	0.17	0.0	0.17	0.0	0.18	0.04	0.17	1.02	1.34
WS <sub>4,8</sub>	0.18	0.18	0.0	0.18	0.0	0.18	0.02	0.18	0.97	1.34
WS <sub>6,2</sub>	0.18	0.19	0.05	0.19	0.05	0.24	0.29	0.18	1.3	1.37
WS <sub>6,4</sub>	0.22	0.22	0.02	0.22	0.02	0.24	0.11	0.22	0.89	1.47
WS <sub>6,6</sub>	0.24	0.24	0.01	0.24	0.01	0.25	0.04	0.24	0.74	1.47
WS <sub>6,8</sub>	0.24	0.25	0.01	0.25	0.01	0.25	0.01	0.24	0.7	1.47
WS <sub>8,2</sub>	0.22	0.23	0.06	0.23	0.06	0.29	0.28	0.22	1.1	1.49
WS <sub>8,4</sub>	0.26	0.27	0.03	0.27	0.03	0.29	0.11	0.26	0.75	1.52
WS <sub>8,6</sub>	0.28	0.29	0.01	0.29	0.01	0.29	0.04	0.28	0.62	1.53
WS <sub>8,8</sub>	0.29	0.29	0.01	0.29	0.01	0.29	0.01	0.29	0.58	1.52

## 2. Lognormal

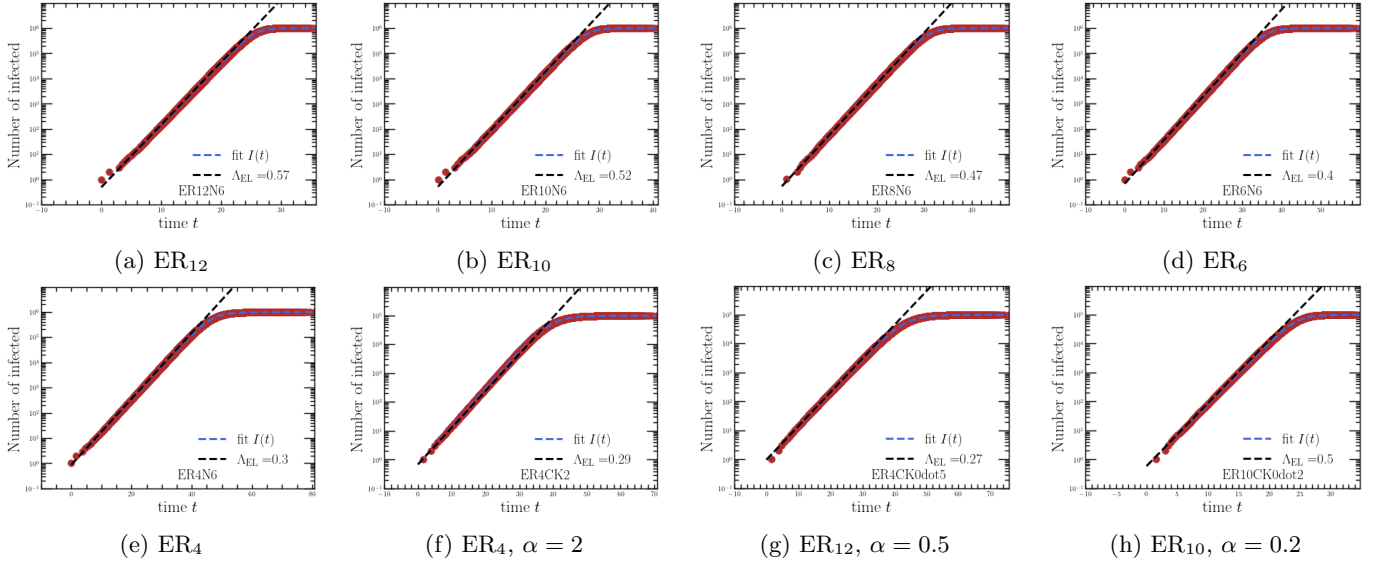


FIG. 9: Average epidemic trajectories on Erdős-Rényi networks from the configuration model with a Lognormal generation-time distribution.

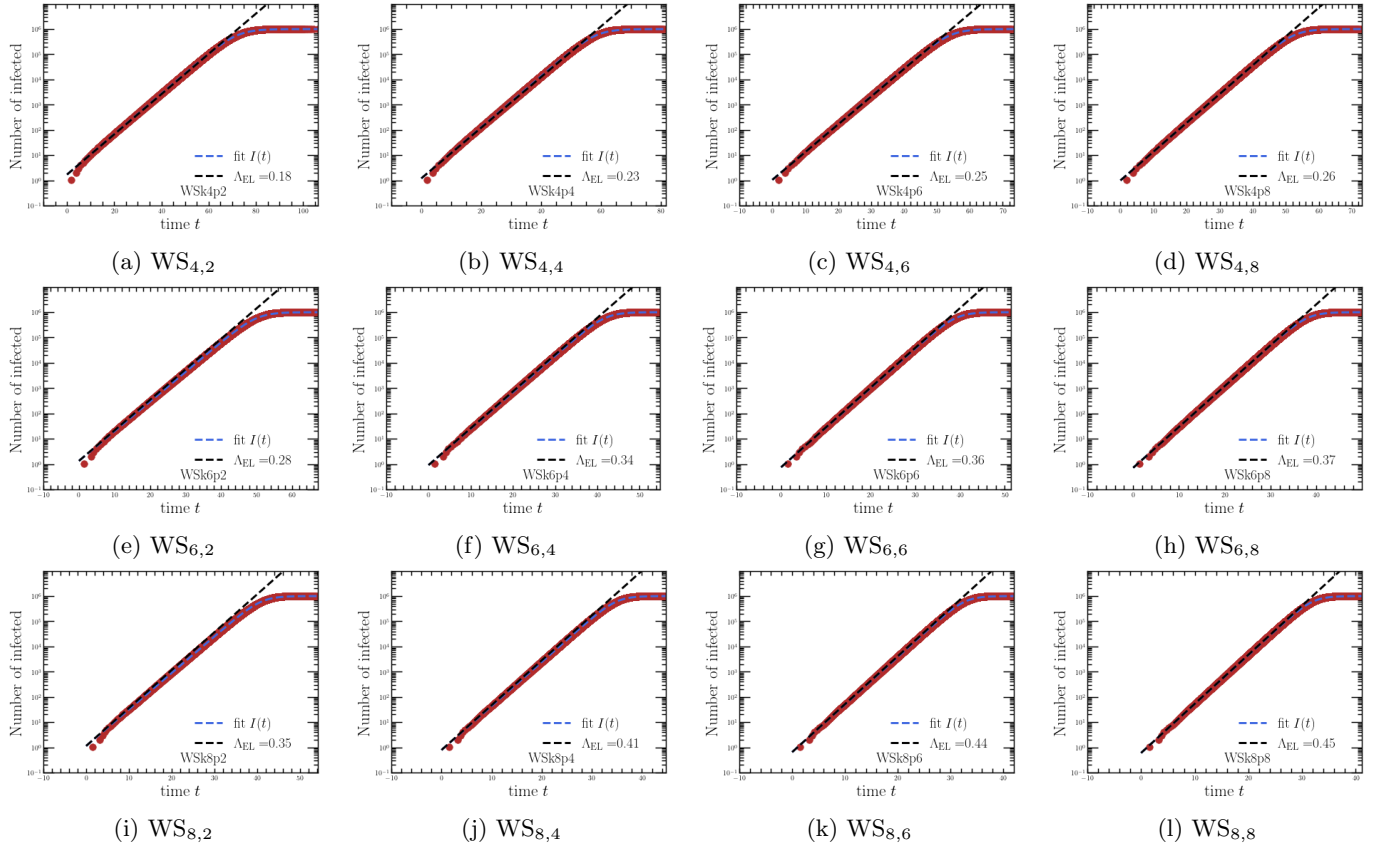


FIG. 10: Average epidemic trajectories on Watts–Strogatz networks with a Lognormal generation-time distribution.

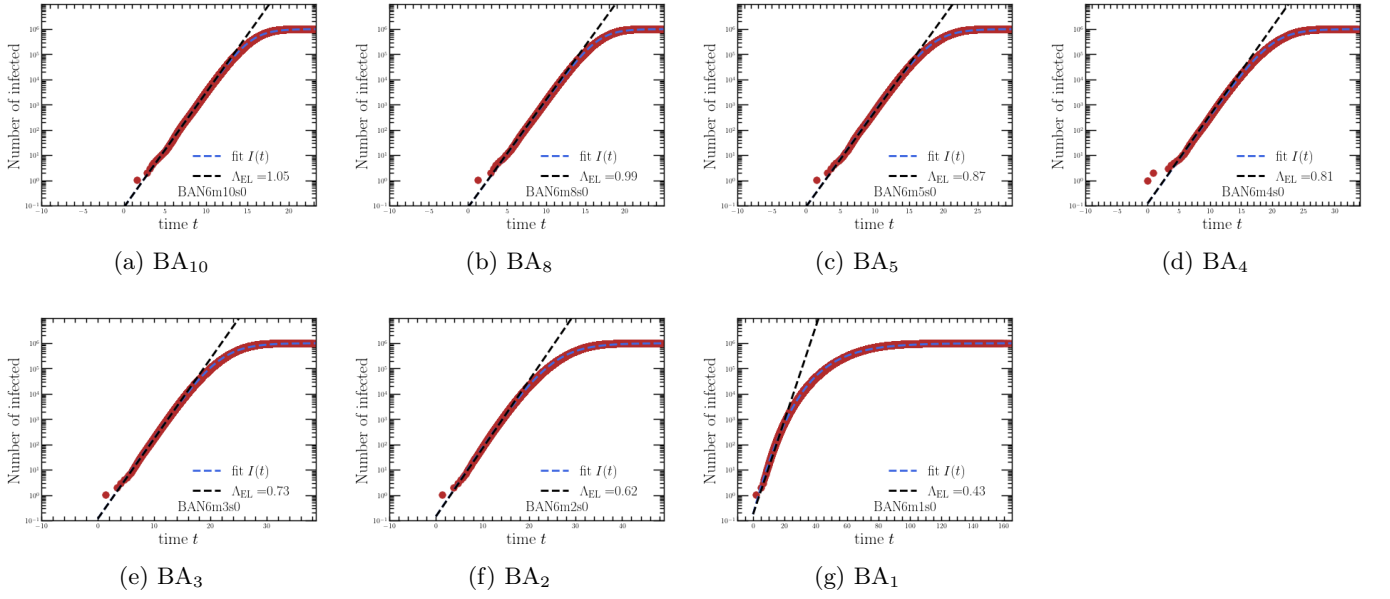


FIG. 11: Average epidemic trajectories on Barabási-Albert networks with a Lognormal generation-time distribution.

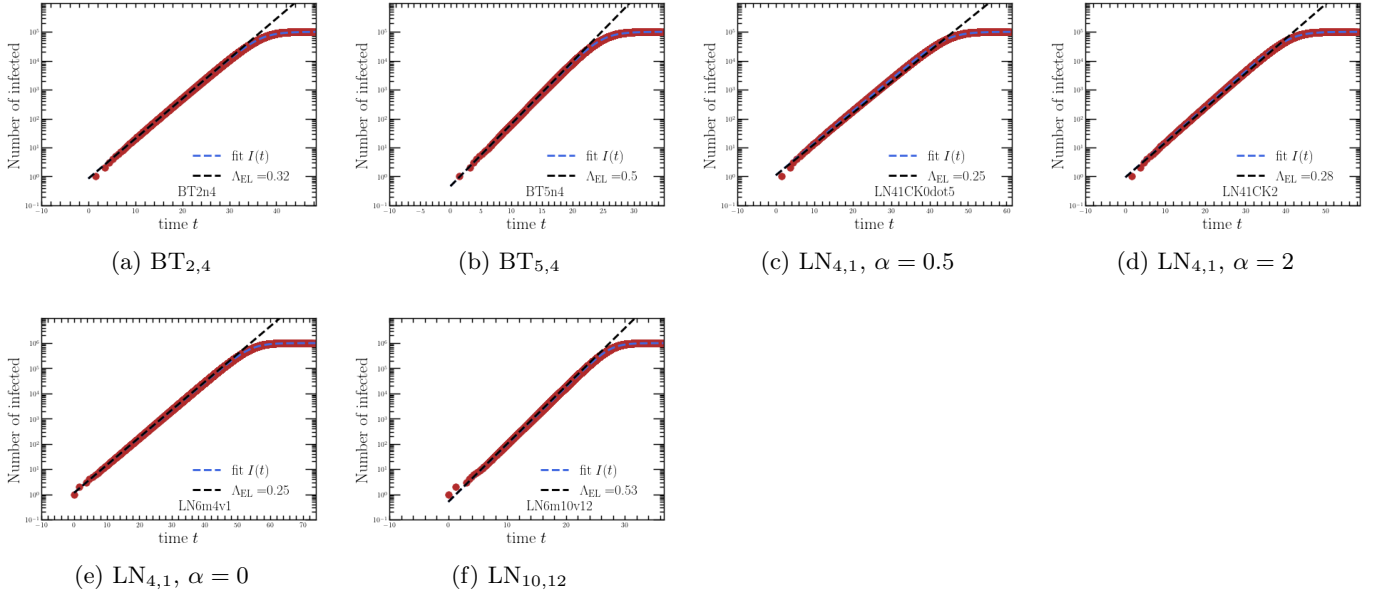


FIG. 12: Average epidemic trajectories on networks from the configuration model with a Lognormal generation-time distribution.

TABLE IV: Results of the fitting procedure for synthetic networks with a Lognormal generation-time distribution

Network	$\Lambda_{\text{FIT}}$	$\Lambda_R$	Error $_R$	$\Lambda_{R_{\text{pert}}}$	Error $_{R_{\text{pert}}}$	$\Lambda_{R_0}$	Error $_{R_0}$	$\Lambda_0$	$I_{0(\text{fit})}$	$\nu$
BA <sub>1</sub>	0.52	0.48	-0.07	0.43	-0.2	0.61	0.16	0.87	0.17	0.06
BA <sub>2</sub>	0.63	0.64	0.01	0.62	-0.02	0.71	0.12	0.63	0.14	0.37
BA <sub>3</sub>	0.74	0.74	0.0	0.73	-0.01	0.8	0.08	0.74	0.12	0.45
BA <sub>4</sub>	0.8	0.81	0.02	0.81	0.01	0.86	0.08	0.8	0.12	0.51
BA <sub>5</sub>	0.88	0.87	-0.01	0.87	-0.01	0.91	0.03	0.88	0.09	0.54
BA <sub>8</sub>	0.98	0.99	0.01	0.99	0.01	1.01	0.03	0.98	0.08	0.67
BA <sub>10</sub>	1.06	1.06	0.0	1.05	-0.0	1.08	0.02	1.06	0.08	0.65
BA <sub>12</sub>	1.1	1.11	0.01	1.11	0.0	1.13	0.02	1.1	0.09	0.69
ER <sub>4</sub>	0.3	0.3	0.01	0.3	0.01	0.3	0.01	0.3	0.87	1.08
ER <sub>6</sub>	0.39	0.4	0.01	0.4	0.01	0.4	0.01	0.39	0.67	1.21
ER <sub>8</sub>	0.47	0.47	0.0	0.47	0.0	0.47	0.0	0.47	0.53	1.22
ER <sub>10</sub>	0.52	0.52	0.01	0.52	0.01	0.52	0.01	0.52	0.51	1.32
ER <sub>12</sub>	0.57	0.57	0.01	0.57	0.01	0.57	0.01	0.57	0.48	1.38
ER <sub>10</sub> $\alpha = 0.2$	0.49	0.5	0.01	0.5	0.02	0.52	0.07	0.49	0.59	1.32
ER <sub>4</sub> $\alpha = 2$	0.3	0.3	-0.01	0.29	-0.03	0.3	-0.0	0.3	0.68	0.97
ER <sub>4</sub> $\alpha = 0.5$	0.27	0.26	-0.01	0.27	0.01	0.3	0.12	0.27	0.97	0.99
LN <sub>4,1</sub> $\alpha = 0.5$	0.25	0.25	-0.04	0.25	-0.03	0.29	0.11	0.25	1.1	1.28
LN <sub>4,1</sub> $\alpha = 2$	0.28	0.28	-0.02	0.28	-0.02	0.29	0.01	0.28	0.93	1.27
BT <sub>2,4</sub>	0.32	0.32	0.0	0.32	0.0	0.32	0.0	0.32	0.84	1.33
BT <sub>5,4</sub>	0.49	0.5	0.01	0.5	0.0	0.5	0.0	0.49	0.46	1.13
LN <sub>10,12</sub>	0.53	0.53	0.01	0.53	0.01	0.53	0.01	0.53	0.5	1.31
LN <sub>4,1</sub>	0.25	0.25	0.0	0.25	0.0	0.25	0.0	0.25	1.14	1.35
WS <sub>4,2</sub>	0.18	0.18	0.0	0.18	-0.01	0.25	0.29	0.18	1.69	1.18
WS <sub>4,4</sub>	0.23	0.23	-0.01	0.23	-0.01	0.26	0.1	0.23	1.19	1.23
WS <sub>4,6</sub>	0.25	0.25	-0.0	0.25	-0.0	0.26	0.04	0.25	1.04	1.25
WS <sub>4,8</sub>	0.26	0.26	-0.0	0.26	-0.0	0.27	0.02	0.26	0.99	1.24
WS <sub>6,2</sub>	0.27	0.28	0.03	0.28	0.03	0.36	0.29	0.27	1.33	1.29
WS <sub>6,4</sub>	0.33	0.34	0.01	0.34	0.01	0.37	0.1	0.33	0.91	1.35
WS <sub>6,6</sub>	0.36	0.36	0.0	0.36	0.0	0.37	0.03	0.36	0.75	1.34
WS <sub>6,8</sub>	0.37	0.37	0.0	0.37	0.0	0.38	0.01	0.37	0.71	1.33
WS <sub>8,2</sub>	0.33	0.35	0.04	0.35	0.04	0.44	0.28	0.33	1.13	1.39
WS <sub>8,4</sub>	0.4	0.41	0.02	0.41	0.02	0.44	0.1	0.4	0.78	1.39
WS <sub>8,6</sub>	0.43	0.44	0.01	0.44	0.01	0.45	0.03	0.43	0.64	1.39
WS <sub>8,8</sub>	0.45	0.45	0.0	0.45	0.0	0.45	0.01	0.45	0.6	1.38



## 3. Weibull

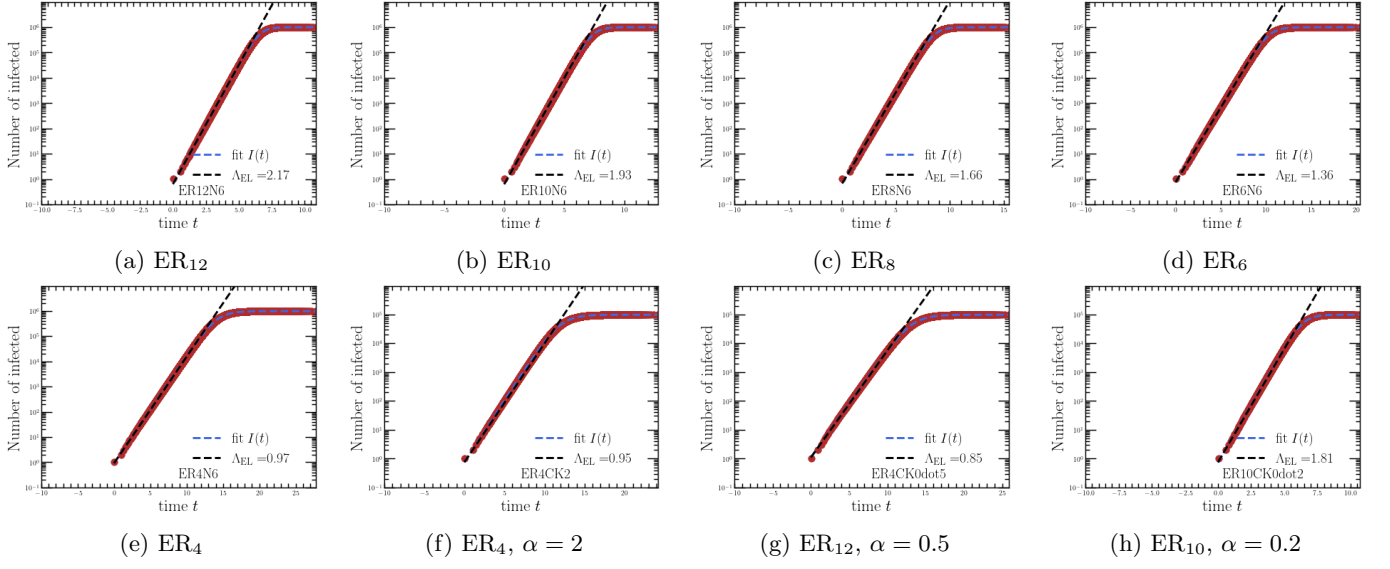


FIG. 13: Average epidemic trajectories on Erdős-Rényi networks with a Weibull generation-time distribution.

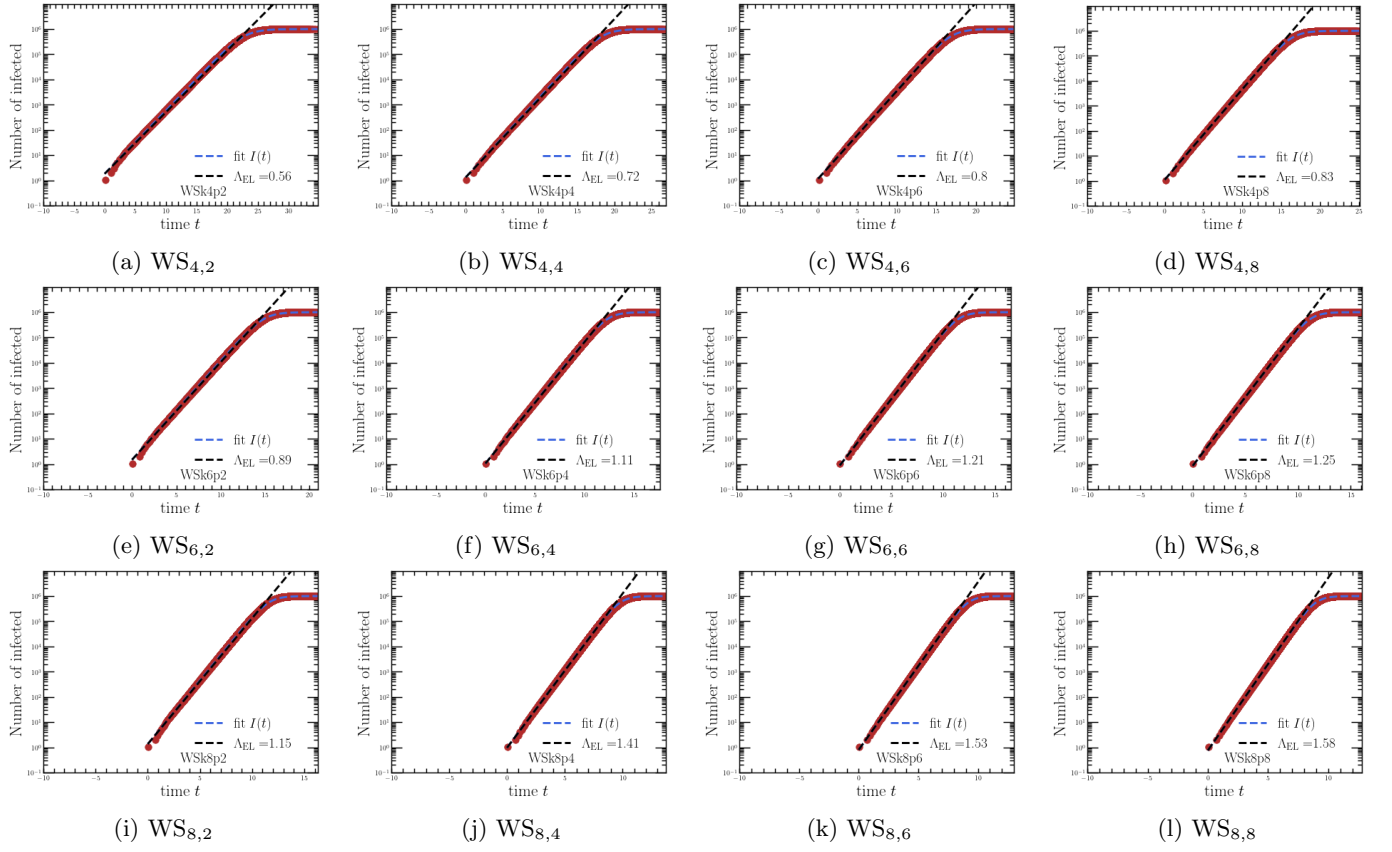


FIG. 14: Average epidemic trajectories on Watts–Strogatz networks with a Weibull generation-time distribution.

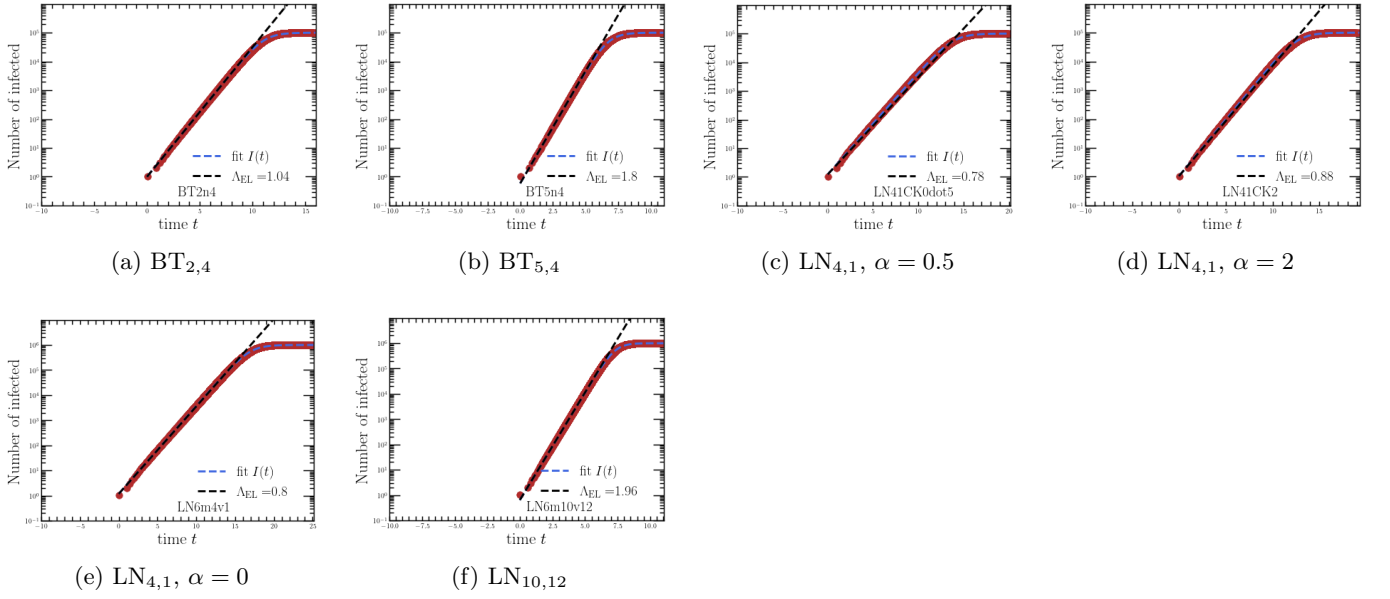


FIG. 15: Average epidemic trajectories on networks from the configuration model with a Weibull generation-time distribution.

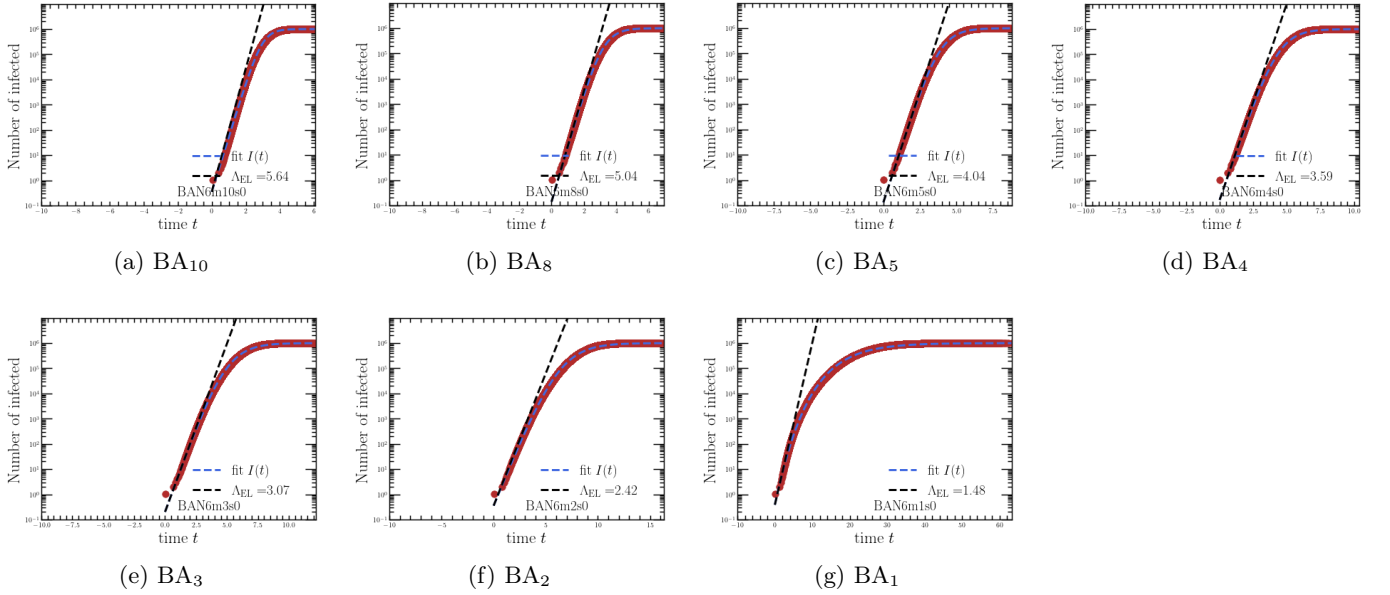


FIG. 16: Average epidemic trajectories on Barabási-Albert networks from the configuration model with a Weibull generation-time distribution.

TABLE V: Results of the fitting procedure for synthetic networks with a Weibull generation-time distribution

Network	$\Lambda_{\text{FIT}}$	$\Lambda_R$	Error $_R$	$\Lambda_{R_{\text{pert}}}$	Error $_{R_{\text{pert}}}$	$\Lambda_{R_0}$	Error $_{R_0}$	$\Lambda_0$	$I_{0(\text{fit})}$	$\nu$
BA <sub>1</sub>	1.6	1.74	0.08	1.48	-0.08	2.37	0.39	5.0	0.38	0.03
BA <sub>2</sub>	2.31	2.53	0.09	2.42	0.05	2.97	0.25	2.35	0.35	0.27
BA <sub>3</sub>	3.1	3.15	0.02	3.07	-0.01	3.54	0.13	3.14	0.2	0.28
BA <sub>4</sub>	3.54	3.65	0.03	3.59	0.01	3.98	0.12	3.57	0.17	0.31
BA <sub>5</sub>	4.1	4.07	-0.01	4.04	-0.01	4.36	0.06	4.12	0.13	0.32
BA <sub>8</sub>	4.98	5.08	0.02	5.04	0.01	5.27	0.06	5.0	0.14	0.36
BA <sub>10</sub>	5.0	5.69	0.13	5.64	0.12	5.88	0.16	5.0	0.35	0.52
ER <sub>4</sub>	0.98	0.97	-0.01	0.97	-0.01	0.97	-0.01	0.98	0.92	0.88
ER <sub>6</sub>	1.36	1.36	-0.0	1.36	-0.0	1.36	-0.0	1.36	0.76	0.97
ER <sub>8</sub>	1.67	1.66	-0.0	1.66	-0.0	1.66	-0.0	1.67	0.67	1.0
ER <sub>10</sub>	1.93	1.93	0.0	1.93	0.0	1.93	0.0	1.93	0.63	1.02
ER <sub>12</sub>	2.16	2.17	0.0	2.17	0.0	2.17	0.0	2.16	0.63	1.07
ER <sub>10</sub> $\alpha = 0.2$	1.83	1.8	-0.02	1.81	-0.01	1.93	0.06	1.83	0.75	1.06
ER <sub>4</sub> $\alpha = 2$	0.98	0.96	-0.02	0.95	-0.04	0.97	-0.01	0.98	0.75	0.83
ER <sub>4</sub> $\alpha = 0.5$	0.86	0.84	-0.03	0.85	-0.01	0.97	0.12	0.86	1.1	0.85
LN <sub>4,1</sub> $\alpha = 0.5$	0.82	0.77	-0.05	0.78	-0.05	0.91	0.11	0.82	1.23	1.13
LN <sub>4,1</sub> $\alpha = 2$	0.9	0.88	-0.02	0.88	-0.03	0.91	0.01	0.9	1.05	1.09
BT <sub>2,4</sub>	1.04	1.04	-0.0	1.04	-0.0	1.04	-0.0	1.04	0.99	1.13
BT <sub>5,4</sub>	1.8	1.81	0.0	1.8	0.0	1.8	0.0	1.8	0.59	0.88
LN <sub>10,12</sub>	1.96	1.96	0.0	1.96	0.0	1.96	0.0	1.96	0.64	1.01
LN <sub>4,1</sub>	0.81	0.8	-0.01	0.8	-0.01	0.8	-0.01	0.81	1.17	1.11
WS <sub>4,2</sub>	0.58	0.56	-0.03	0.56	-0.03	0.78	0.3	0.58	1.81	1.1
WS <sub>4,4</sub>	0.74	0.72	-0.02	0.72	-0.02	0.81	0.1	0.74	1.31	1.1
WS <sub>4,6</sub>	0.81	0.8	-0.01	0.8	-0.01	0.84	0.04	0.81	1.16	1.1
WS <sub>4,8</sub>	0.84	0.83	-0.0	0.83	-0.0	0.85	0.02	0.84	1.1	1.08
WS <sub>6,2</sub>	0.9	0.89	-0.01	0.89	-0.01	1.21	0.29	0.9	1.48	1.15
WS <sub>6,4</sub>	1.11	1.11	-0.01	1.11	-0.01	1.23	0.1	1.11	1.05	1.16
WS <sub>6,6</sub>	1.21	1.21	-0.0	1.21	-0.0	1.25	0.03	1.21	0.88	1.13
WS <sub>6,8</sub>	1.25	1.25	0.0	1.25	0.0	1.26	0.01	1.25	0.85	1.13
WS <sub>8,2</sub>	1.16	1.15	-0.01	1.15	-0.01	1.54	0.28	1.16	1.34	1.2
WS <sub>8,4</sub>	1.42	1.41	-0.01	1.41	-0.0	1.56	0.1	1.42	0.96	1.17
WS <sub>8,6</sub>	1.53	1.53	-0.0	1.53	0.0	1.58	0.03	1.53	0.79	1.15
WS <sub>8,8</sub>	1.58	1.58	0.0	1.58	0.0	1.59	0.01	1.58	0.75	1.13

## F. Trajectories real networks

### 1. Lognormal

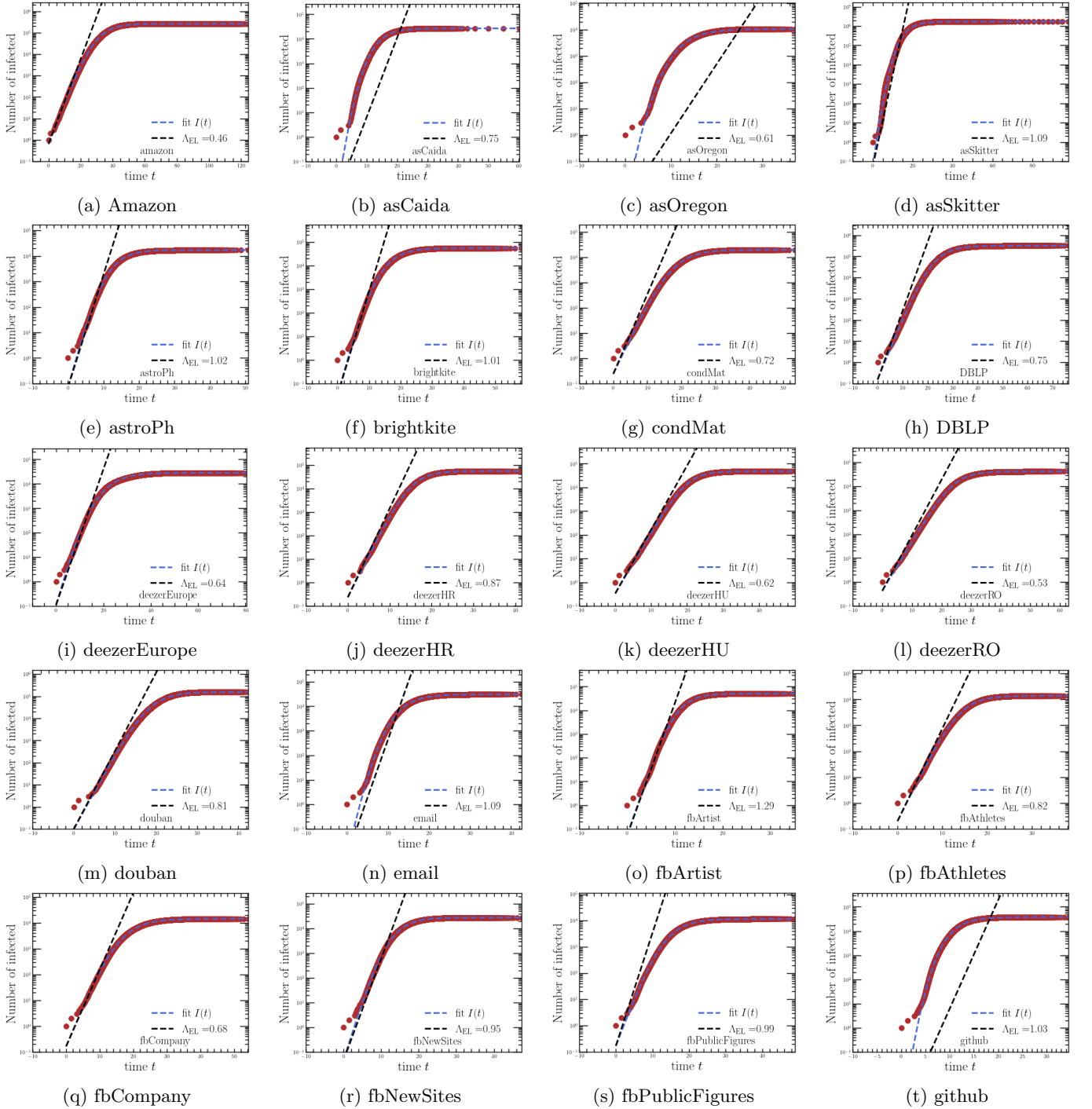


FIG. 17: Average epidemic trajectories on real-world networks with a Lognormal generation-time distribution (I).

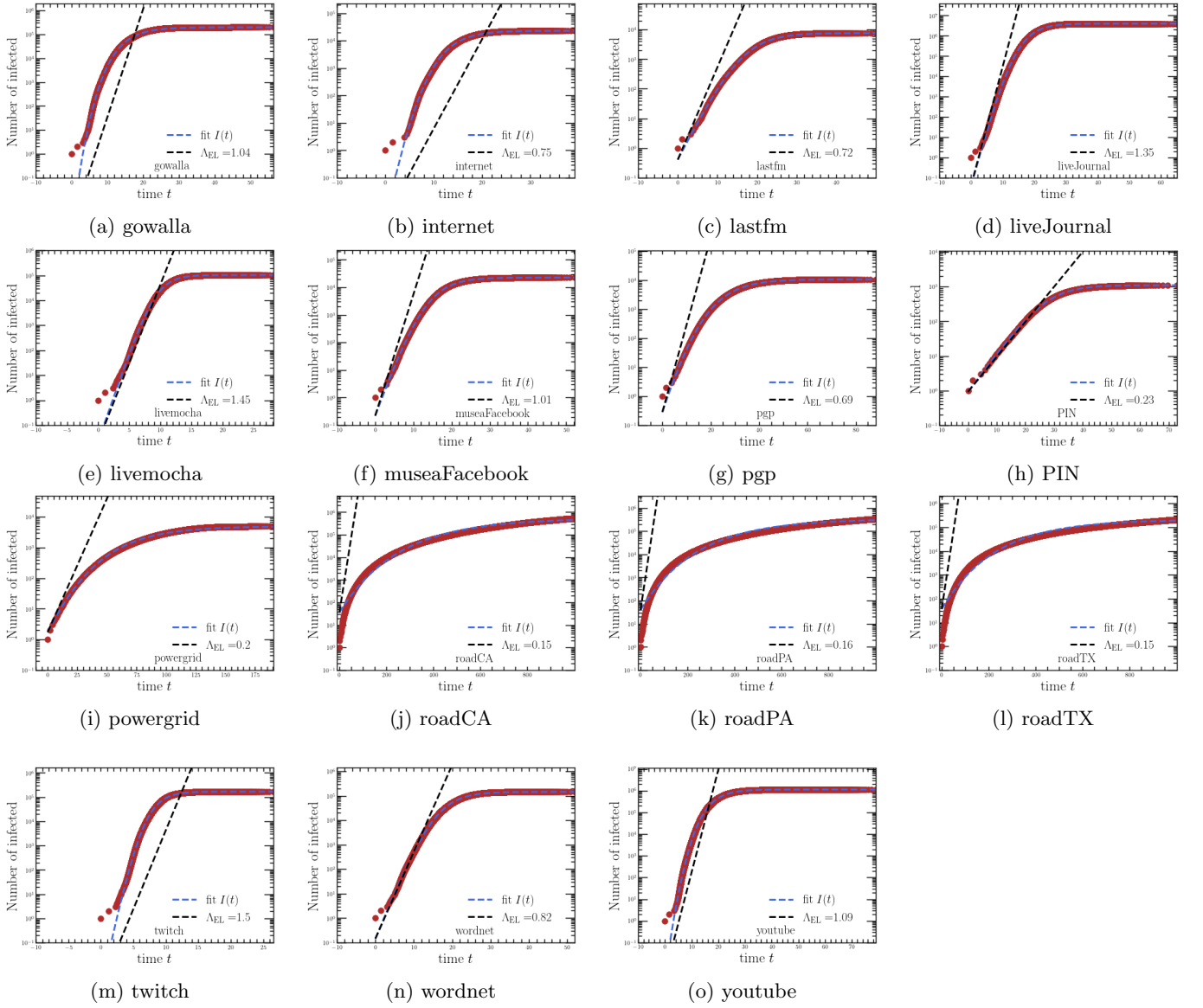


FIG. 18: Average epidemic trajectories on real-world networks with a Lognormal generation-time distribution (II).

TABLE VI: Results and parameters from the fitting procedure on real-world networks with a Lognormal generation-time distribution.

Network	$\Lambda_{\text{FIT}}$	$\Lambda_R$	Error $_R$	$\Lambda_{R_{\text{pert}}}$	Error $_{R_{\text{pert}}}$	$\Lambda_{R_0}$	Error $_{R_0}$	$\Lambda_0$	$I_{0(\text{fit})}$	$\nu$	$\eta$
amazon	0.44	0.46	0.04	0.46	0.02	0.53	0.17	0.45	0.64	0.33	0.01
asCaida	1.74	0.93	-0.61	0.75	-0.8	1.51	-0.14	2.0	0.0	0.13	0.13
asOregon	1.88	0.83	-0.78	0.61	-1.03	1.47	-0.24	2.29	0.0	0.11	0.18
asSkitter	1.64	1.55	-0.06	1.09	-0.4	2.1	0.25	1.87	0.05	0.12	0.12
astroPh	1.15	0.98	-0.15	1.02	-0.12	1.04	-0.09	1.2	0.07	0.25	0.05
brightkite	1.11	0.99	-0.12	1.01	-0.09	1.03	-0.07	1.18	0.03	0.2	0.05
condMat	0.65	0.7	0.08	0.72	0.11	0.72	0.11	0.66	0.24	0.36	0.02
DBLP	0.66	0.68	0.03	0.75	0.12	0.72	0.08	0.67	0.16	0.32	0.01
deezerEurope	0.76	0.64	-0.17	0.64	-0.17	0.63	-0.18	0.83	0.11	0.19	0.09
deezerHR	0.81	0.87	0.07	0.87	0.07	0.86	0.06	0.82	0.23	0.45	0.0
deezerHU	0.59	0.62	0.05	0.62	0.05	0.61	0.04	0.59	0.33	0.57	0.0
deezerRO	0.48	0.53	0.11	0.53	0.12	0.53	0.1	0.48	0.43	0.55	0.0
douban	0.78	0.84	0.08	0.81	0.05	0.87	0.11	0.78	0.1	0.4	0.0
email	1.6	1.12	-0.35	1.09	-0.38	1.28	-0.22	1.76	0.01	0.16	0.09
fbArtist	1.36	1.29	-0.06	1.29	-0.06	1.32	-0.03	1.38	0.05	0.31	0.01
fbAthletes	0.8	0.82	0.03	0.82	0.03	0.88	0.1	0.8	0.2	0.43	0.01
fbCompany	0.72	0.68	-0.05	0.68	-0.05	0.72	0.01	0.74	0.16	0.3	0.03
fbNewSites	1.11	0.95	-0.16	0.95	-0.16	0.96	-0.15	1.15	0.05	0.26	0.03
fbPublicFigures	0.83	0.98	0.16	0.99	0.17	0.96	0.15	0.86	0.17	0.31	0.03
github	2.89	1.2	-0.83	1.03	-0.94	1.67	-0.54	3.34	0.0	0.1	0.13
gowalla	2.5	1.22	-0.69	1.04	-0.83	1.54	-0.48	4.02	0.0	0.05	0.38
internet	1.76	0.93	-0.61	0.75	-0.81	1.49	-0.17	2.03	0.0	0.13	0.13
lastfm	0.59	0.67	0.14	0.72	0.2	0.76	0.26	0.61	0.41	0.35	0.03
liveJournal	1.27	1.35	0.06	1.35	0.06	1.24	-0.03	1.31	0.04	0.19	0.03
livemocha	1.65	1.47	-0.12	1.45	-0.13	1.56	-0.06	1.66	0.02	0.35	0.0
museaFacebook	0.84	0.97	0.14	1.01	0.18	1.02	0.19	0.88	0.22	0.27	0.05
pgp	0.57	0.59	0.03	0.69	0.19	0.68	0.17	0.7	0.28	0.16	0.18
PIN	0.25	0.29	0.13	0.23	-0.09	0.38	0.38	0.26	0.92	0.63	0.01
powergrid	0.18	0.2	0.1	0.2	0.13	0.22	0.24	0.35	1.73	0.09	0.5
roadCA	0.04	0.16	1.21	0.15	1.19	0.16	1.23	5.0	35.48	0.0	0.99
roadPA	0.04	0.15	1.21	0.16	1.21	0.17	1.25	5.0	39.43	0.0	0.99
roadTX	0.04	0.16	1.21	0.15	1.19	0.16	1.23	5.0	36.7	0.0	0.99
twitch	2.76	1.67	-0.49	1.5	-0.59	2.06	-0.29	2.82	0.0	0.21	0.02
wordnet	0.87	0.88	0.02	0.82	-0.06	0.99	0.13	0.89	0.14	0.28	0.02
youtube	1.92	1.27	-0.41	1.09	-0.55	1.71	-0.12	2.39	0.0	0.08	0.2

## 2. Gamma

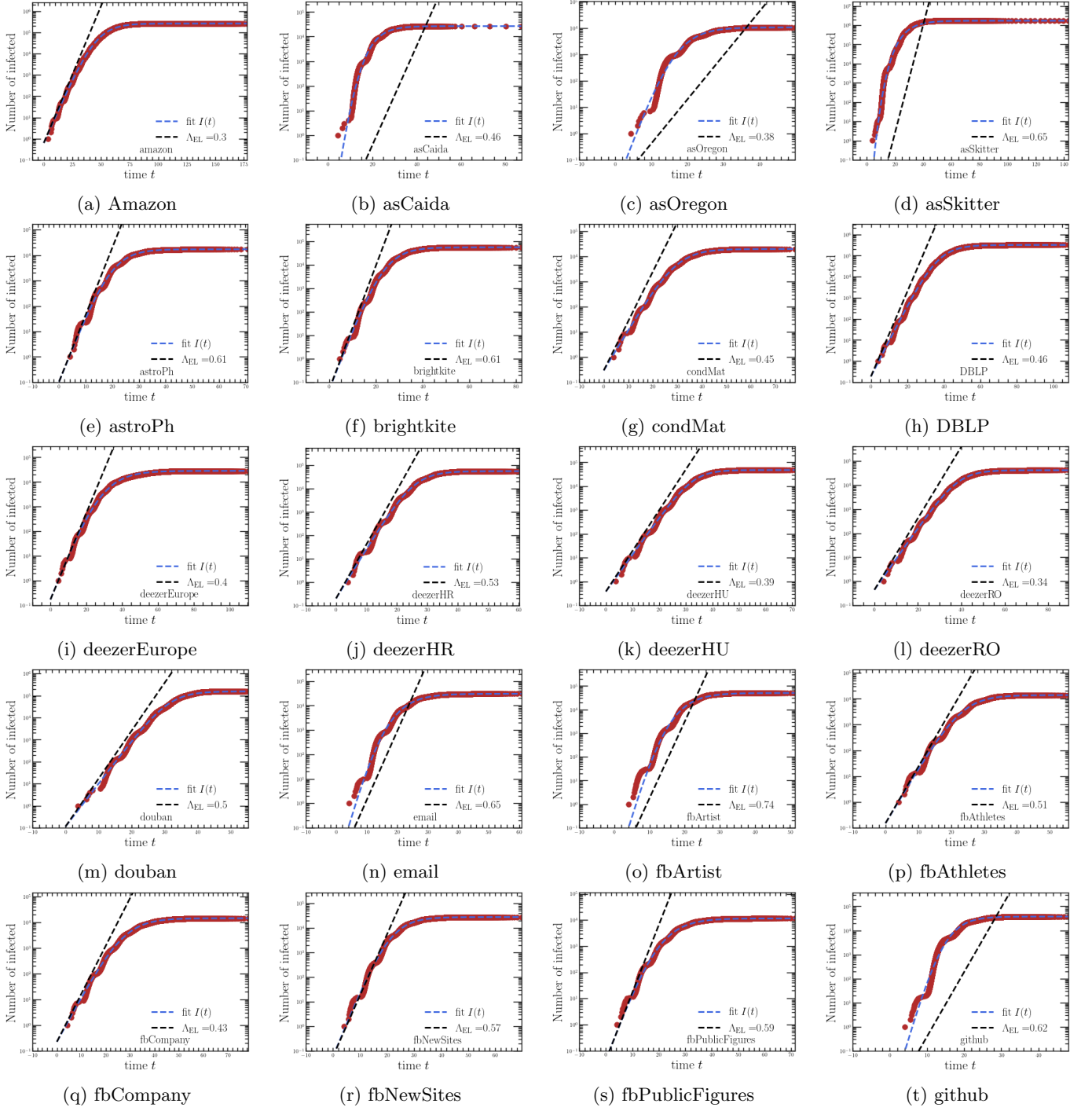


FIG. 19: Average epidemic trajectories on real-world networks with a Gamma generation-time distribution (I).



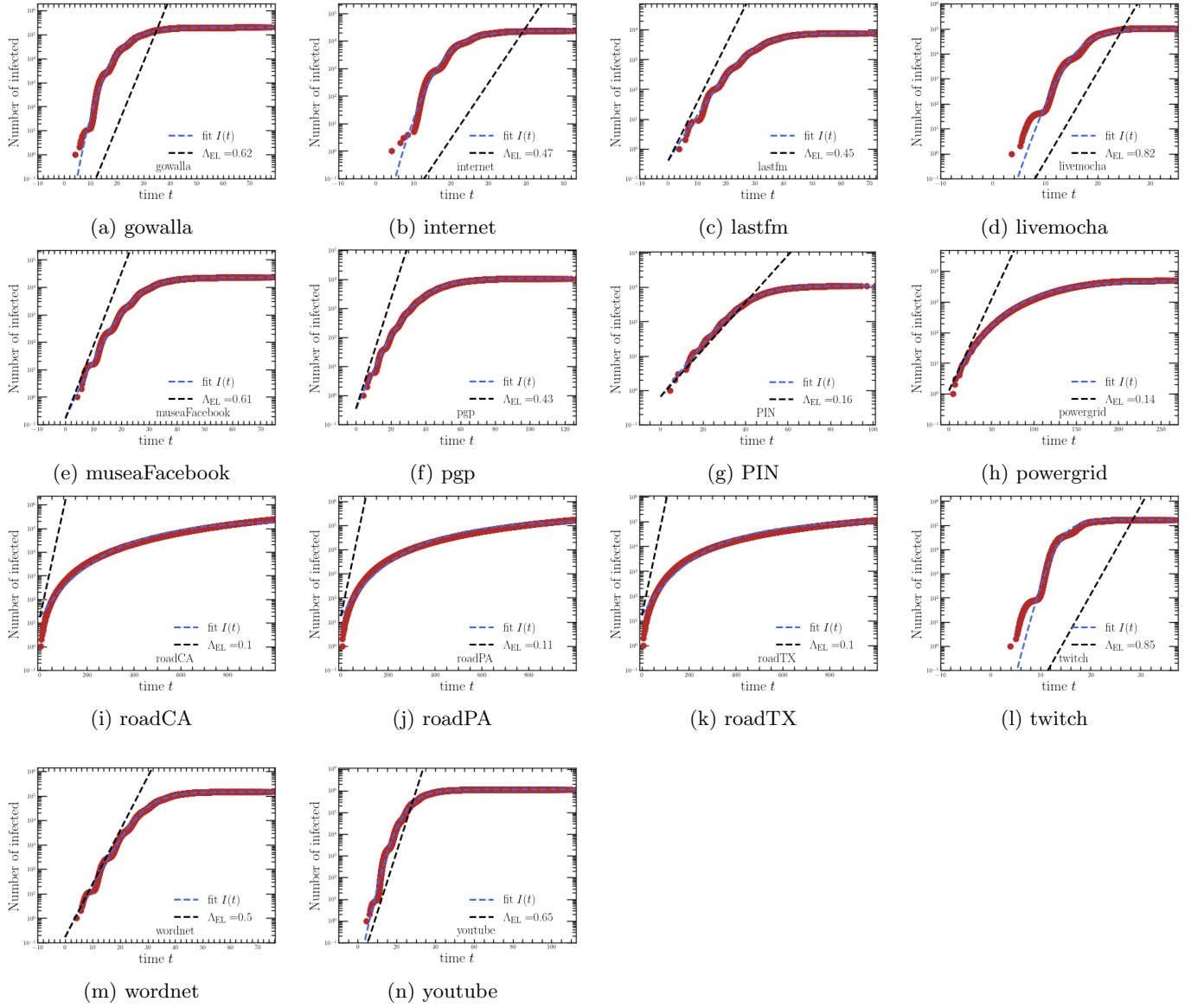


FIG. 20: Average epidemic trajectories on real-world networks with a Gamma generation-time distribution (I).

TABLE VII: Results and parameters from the fitting procedure on real-world networks with a Gamma generation-time distribution.

Network	$\Lambda_{\text{FIT}}$	$\Lambda_R$	Error <sub>R</sub>	$\Lambda_{R_{\text{pert}}}$	Error <sub>R<sub>pert</sub></sub>	$\Lambda_{R_0}$	Error <sub>R<sub>0</sub></sub>	$\Lambda_0$	$I_{0(\text{fit})}$	$\nu$	$\eta$
amazon	0.28	0.3	0.07	0.3	0.06	0.34	0.19	0.28	0.64	0.36	0.01
asCaida	1.45	0.56	-0.89	0.46	-1.03	0.85	-0.52	1.59	0.0	0.12	0.09
asOregon	0.83	0.51	-0.48	0.38	-0.73	0.84	0.01	0.85	0.01	0.27	0.02
asSkitter	2.31	0.87	-0.9	0.65	-1.12	1.12	-0.69	5.0	0.0	0.02	0.54
astroPh	0.6	0.59	-0.01	0.61	0.02	0.62	0.04	0.61	0.11	0.34	0.02
brightkite	0.58	0.59	0.02	0.61	0.05	0.62	0.06	0.59	0.05	0.31	0.01
condMat	0.37	0.44	0.17	0.45	0.2	0.45	0.19	0.37	0.3	0.47	0.01
DBLP	0.39	0.43	0.09	0.46	0.17	0.45	0.14	0.39	0.19	0.4	0.0
deezerEurope	0.42	0.4	-0.03	0.4	-0.03	0.4	-0.04	0.43	0.17	0.27	0.04
deezerHR	0.49	0.53	0.09	0.53	0.09	0.53	0.08	0.49	0.2	0.49	0.0
deezerHU	0.36	0.39	0.1	0.39	0.09	0.39	0.09	0.36	0.38	0.67	0.0
deezerRO	0.3	0.34	0.14	0.34	0.15	0.34	0.13	0.3	0.44	0.62	0.0
douban	0.45	0.51	0.13	0.5	0.11	0.53	0.17	0.45	0.11	0.56	0.0
email	1.0	0.66	-0.41	0.65	-0.43	0.74	-0.3	1.05	0.0	0.18	0.05
fbArtist	1.16	0.75	-0.43	0.74	-0.44	0.76	-0.42	1.2	0.0	0.19	0.04
fbAthletes	0.49	0.51	0.03	0.51	0.03	0.54	0.09	0.49	0.15	0.46	0.01
fbCompany	0.4	0.43	0.07	0.43	0.07	0.45	0.12	0.4	0.23	0.41	0.01
fbNewSites	0.61	0.57	-0.06	0.57	-0.06	0.58	-0.05	0.62	0.06	0.33	0.01
fbPublicFigures	0.61	0.59	-0.03	0.59	-0.02	0.58	-0.04	0.63	0.04	0.26	0.04
github	1.2	0.7	-0.53	0.62	-0.64	0.93	-0.26	1.22	0.0	0.24	0.01
gowalla	1.7	0.71	-0.82	0.62	-0.93	0.87	-0.65	2.28	0.0	0.06	0.26
internet	1.23	0.56	-0.74	0.47	-0.9	0.84	-0.38	1.32	0.0	0.15	0.07
lastfm	0.35	0.42	0.18	0.45	0.23	0.47	0.28	0.36	0.4	0.41	0.02
livemocha	1.44	0.84	-0.53	0.82	-0.55	0.88	-0.49	1.47	0.0	0.2	0.02
museaFacebook	0.5	0.58	0.15	0.61	0.19	0.61	0.19	0.52	0.17	0.31	0.03
pgp	0.32	0.37	0.15	0.43	0.29	0.42	0.27	0.35	0.34	0.24	0.09
PIN	0.18	0.19	0.07	0.16	-0.14	0.25	0.31	0.18	0.65	0.61	0.01
powergrid	0.13	0.13	-0.0	0.14	0.02	0.15	0.13	0.32	1.27	0.06	0.59
roadCA	0.03	0.11	1.02	0.1	1.0	0.11	1.04	5.0	17.23	0.0	0.99
roadPA	0.04	0.11	0.98	0.11	0.99	0.11	1.03	5.0	17.25	0.0	0.99
roadTX	0.04	0.11	0.99	0.1	0.96	0.11	1.0	5.0	16.23	0.0	0.99
twitch	1.86	0.93	-0.67	0.85	-0.75	1.1	-0.51	1.86	0.0	0.25	0.0
wordnet	0.49	0.54	0.09	0.5	0.02	0.6	0.19	0.5	0.17	0.34	0.01
youtube	0.99	0.74	-0.29	0.65	-0.42	0.94	-0.04	1.06	0.0	0.13	0.07

## 3. Weibull

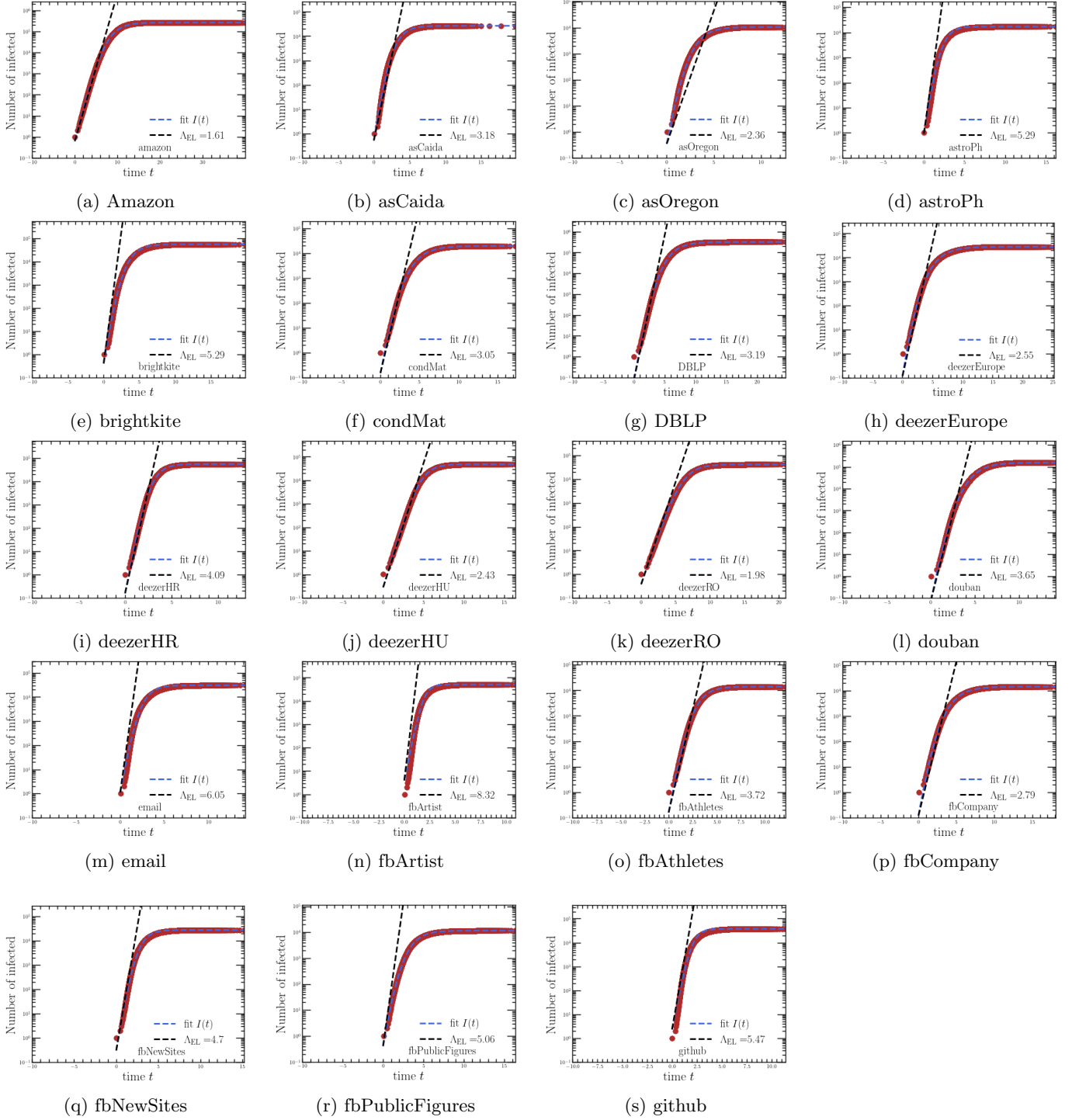


FIG. 21: Average epidemic trajectories on real-world networks with a Weibull generation-time distribution (I).

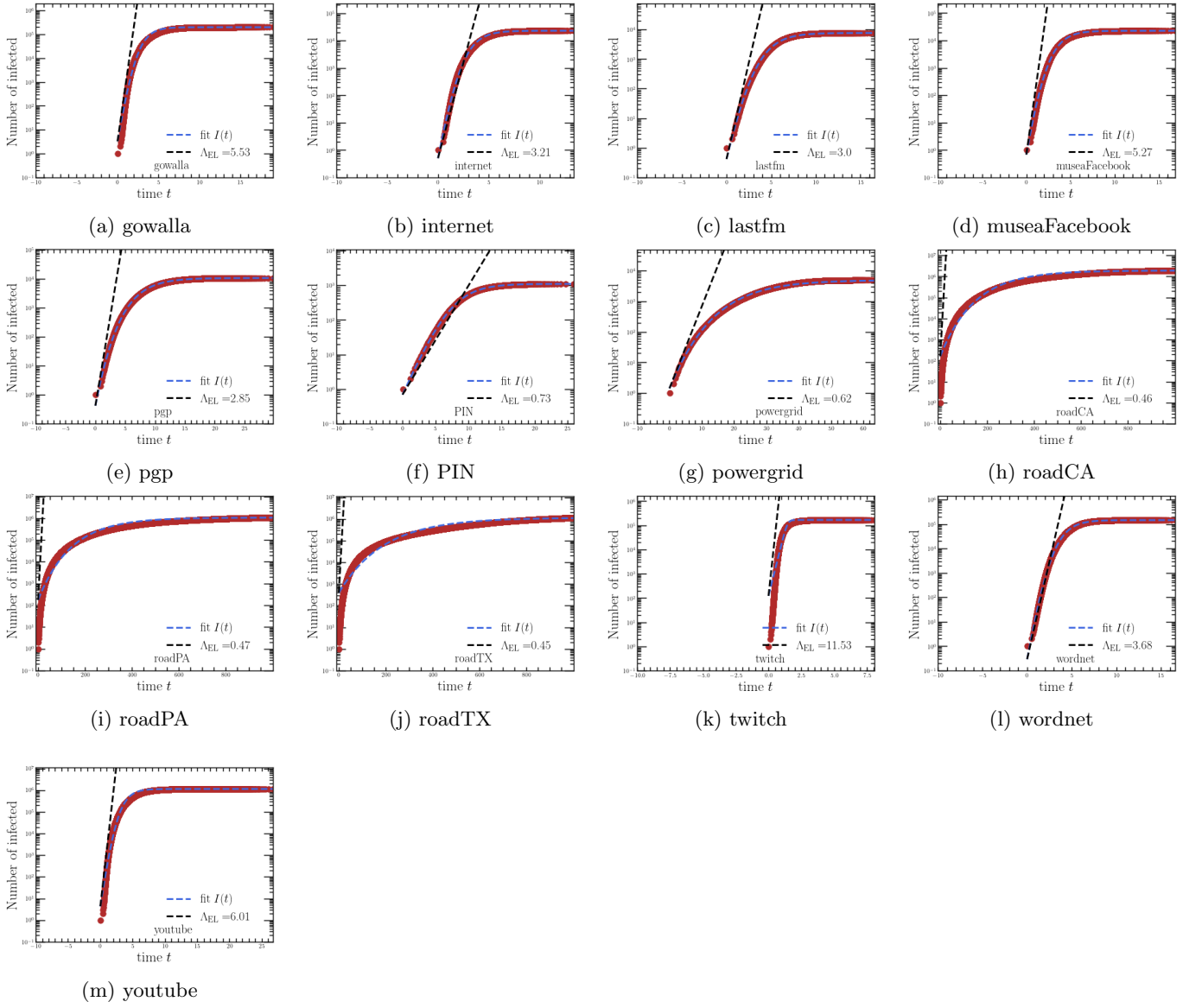


FIG. 22: Average epidemic trajectories on real-world networks with a Weibull generation-time distribution (I).

TABLE VIII: Results and parameters from the fitting procedure on real-world networks with a Weibull generation-time distribution.

Network	$\Lambda_{\text{FIT}}$	$\Lambda_R$	Error <sub>R</sub>	$\Lambda_{R_{\text{pert}}}$	Error <sub>R<sub>pert</sub></sub>	$\Lambda_{R_0}$	Error <sub>R<sub>0</sub></sub>	$\Lambda_0$	$I_{0(\text{fit})}$	$\nu$	$\eta$
amazon	1.77	1.65	-0.08	1.61	-0.1	1.95	0.09	1.84	0.62	0.26	0.03
asCaida	4.27	4.51	0.06	3.18	-0.29	11.75	0.93	5.0	0.52	0.18	0.15
asOregon	4.21	3.77	-0.11	2.36	-0.57	11.14	0.9	5.0	0.35	0.18	0.16
asSkitter	4.8	12.43	0.89	6.02	0.23	26.84	1.39	5.0	14.54	0.27	0.04
astroPh	4.58	4.98	0.08	5.29	0.14	5.54	0.19	5.0	0.92	0.25	0.08
brightkite	4.3	5.03	0.15	5.29	0.21	5.47	0.24	5.0	0.41	0.17	0.14
condMat	3.74	2.91	-0.25	3.05	-0.2	3.03	-0.21	4.64	0.15	0.14	0.19
DBLP	3.64	2.79	-0.26	3.19	-0.13	3.0	-0.19	4.08	0.08	0.15	0.11
deezerEurope	3.52	2.53	-0.33	2.55	-0.32	2.5	-0.34	5.0	0.12	0.1	0.3
deezerHR	4.77	4.08	-0.16	4.09	-0.15	4.0	-0.17	5.0	0.16	0.24	0.05
deezerHU	2.62	2.44	-0.07	2.43	-0.07	2.4	-0.08	2.64	0.28	0.38	0.01
deezerRO	1.95	1.96	0.01	1.98	0.02	1.94	-0.0	1.97	0.38	0.38	0.01
douban	4.4	3.82	-0.14	3.65	-0.19	4.07	-0.08	5.0	0.08	0.15	0.12
email	4.5	6.35	0.34	6.05	0.29	8.25	0.59	5.0	1.1	0.23	0.1
fbArtist	4.93	8.35	0.51	8.32	0.51	8.74	0.56	5.0	3.91	0.46	0.01
fbAthletes	4.55	3.72	-0.2	3.72	-0.2	4.16	-0.09	5.0	0.16	0.21	0.09
fbCompany	3.86	2.77	-0.33	2.79	-0.32	3.02	-0.24	5.0	0.12	0.13	0.23
fbNewSites	4.67	4.72	0.01	4.7	0.01	4.83	0.03	5.0	0.3	0.24	0.07
fbPublicFigures	4.05	4.93	0.2	5.06	0.22	4.84	0.18	5.0	0.41	0.16	0.19
github	4.87	7.21	0.39	5.47	0.12	14.78	1.01	5.0	2.31	0.37	0.03
gowalla	4.43	7.49	0.51	5.53	0.22	12.3	0.94	5.0	3.27	0.2	0.11
internet	4.29	4.58	0.07	3.21	-0.29	11.35	0.9	5.0	0.51	0.18	0.14
lastfm	2.82	2.74	-0.03	3.0	0.06	3.29	0.15	3.4	0.42	0.18	0.17
livemocha	5.0	11.14	0.76	10.74	0.73	12.72	0.87	5.0	15.26	0.82	0.0
museaFacebook	4.09	4.87	0.17	5.27	0.25	5.35	0.27	5.0	0.68	0.16	0.18
pgp	2.4	2.26	-0.06	2.85	0.17	2.75	0.14	5.0	0.42	0.06	0.52
PIN	0.95	0.94	-0.02	0.73	-0.27	1.27	0.28	1.01	0.69	0.4	0.05
powergrid	0.59	0.6	0.02	0.62	0.05	0.7	0.17	1.67	1.43	0.05	0.65
roadCA	0.06	0.47	1.52	0.46	1.51	0.49	1.53	5.0	161.13	0.0	0.99
roadPA	0.06	0.46	1.53	0.47	1.53	0.5	1.56	5.0	175.98	0.0	0.99
roadTX	0.04	0.47	1.68	0.45	1.66	0.48	1.68	5.0	392.36	0.0	0.99
twitch	5.0	14.8	0.99	11.53	0.79	25.47	1.34	5.0	122.42	1.56	0.0
wordnet	4.42	4.18	-0.06	3.68	-0.18	5.08	0.14	5.0	0.29	0.16	0.12
youtube	4.44	8.12	0.59	6.01	0.3	15.66	1.12	5.0	4.37	0.17	0.11

### G. Comparison between estimates of the reproduction number

It is possible, in principle, to use  $R_0$  instead of  $R_{\text{pert}}$  to predict the spreading rate by means of the network Euler-Lotka equation. We here test the performance of this simpler approach.

For synthetic networks, the predictions of  $\Lambda$  by the network Euler-Lotka equation using  $R_{\text{pert}}$  as the reproduction number are very accurate (Fig. 23a). In contrast, using  $R_0$  leads to an overestimate of the spreading rates (Fig. 23b). The reason is that  $R_0$  tends to over-estimate the reproduction number (see Table 1 in the Main Text), most noticeably for Barabási-Albert and Watts–Strogatz networks. The relative errors on  $\Lambda$  using  $R_{\text{pert}}$  and  $R_0$  for different synthetic networks and generation time distributions are listed in Tables III, IV, and V.

For real-world networks, the predictions of  $\Lambda$  using  $R_{\text{pert}}$  are more accurate on average than those using  $R_0$ , as long as  $\eta < 0.5$  (see Fig. 24a). For larger values of  $\eta$ ,  $R_0$  provides slightly more accurate predictions of the spreading rate (Fig. 24a), although  $R_{\text{pert}}$  still provides a better estimate of the reproduction number (Fig. 24b). As discussed in the Main Text, this suggests a compensatory effect acting for large  $\eta$ . Examples of comparison between the exponential spreading rates estimated using  $R_{\text{pert}}$  and  $R_0$  are shown in Fig. 25

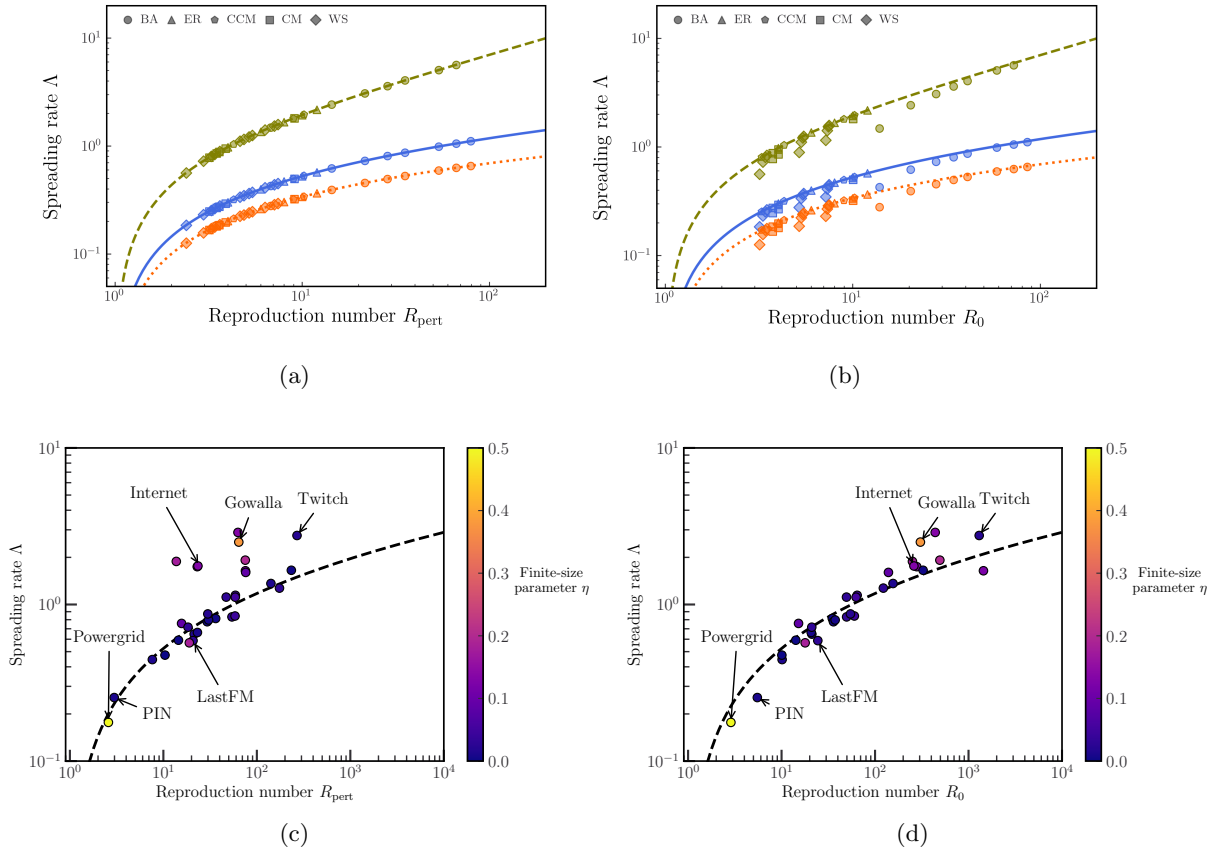


FIG. 23: **Comparison of the prediction of the spreading rate using different estimates of the reproduction number.** (a) Same as Fig. 2c in the Main Text. (b) Same as Fig. 2c in the Main Text, but using  $R_0$  instead of  $R_{\text{pert}}$ . (c) Same as Fig. 3c in the Main Text. (d) Same as Fig. 3c in the Main Text, but using  $R_0$  instead of  $R_{\text{pert}}$ .

### V. EXPLICIT CALCULATION OF THE REPRODUCTION NUMBER FOR NETWORKS

In this section, we provide additional details on the calculation of the reproduction number presented in the Methods. In the unperturbed case, the reproduction matrix has a single non-zero eigenvalue  $R_{\text{unper}}$  with left and

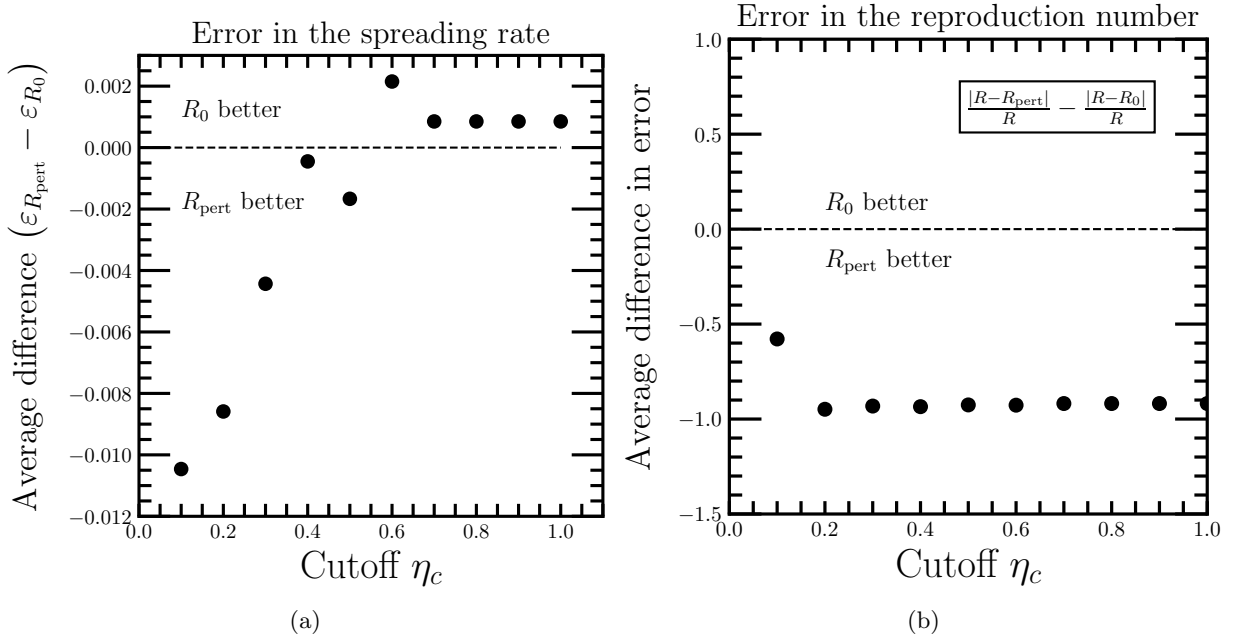


FIG. 24: **Performance of  $R_{\text{pert}}$  and  $R_0$  for different values of the finite-size parameter  $\eta$ .** (a). Mean difference between the relative errors of spreading rates estimated using  $R_{\text{pert}}$  and  $R_0$  as a function of the finite-size parameter  $\eta$ . Each dot represents the average of  $\varepsilon_{R_{\text{pert}}} - \varepsilon_{R_0} = 2|\Lambda_{R_{\text{pert}}} - \Lambda_{\text{fit}}|/(\Lambda_{R_{\text{pert}}} + \Lambda_{\text{fit}}) - 2|\Lambda_{R_0} - \Lambda_{\text{fit}}|/(\Lambda_{R_0} + \Lambda_{\text{fit}})$  across all cases where  $\eta \leq \eta_c$ . (b). Mean difference between the errors of  $R_{\text{pert}}$  and  $R_0$  as estimators of the reproduction number  $R$  is a function of the finite-size parameter  $\eta_c$ . Each dot represents the average of  $|R_{\text{pert}} - R|/R - |R_0 - R|/R$  across all cases where  $\eta \leq \eta_c$ .

right eigenvectors  $u_k^{(0)}$  and  $v_k^{(0)}$ , normalised such that  $\sum_k v_k^{(0)} u_k^{(0)} = 1$ :

$$R_{\text{unper}} = \frac{\overline{k^2} - \overline{k}}{\overline{k}} - m_1, \quad (35)$$

$$u_k^{(0)} = \frac{(k-1)(1-c_k)}{R_{\text{unper}}} \quad (36)$$

$$v_k^{(0)} = \frac{k}{\overline{k}} P(k). \quad (37)$$

At the order of  $\mathcal{O}(r)$ , the leading eigenvalue is given by:

$$R_{\text{pert}} = R_{\text{unper}} + r \sum_{kk'} u_k^{(0)} \delta M_{kk'} v_{k'}^{(0)} + \mathcal{O}(r^2), \quad (38)$$

where

$$\sum_{kk'} u_k^{(0)} \delta M_{kk'} v_{k'}^{(0)} = \frac{1}{R_{\text{unper}}} \sum_{kk'} \left[ (k-1)(1-c_k)(k'-1)(1-c(k')) P^{(1)}(k|k') P(k') \frac{k'}{\overline{k}} \right] - R_{\text{unper}}. \quad (39)$$

Expanding the terms involving clustering coefficients, we separate the sum in four distinct terms. The first three are

$$\sum_{kk'} (k-1)(k'-1) P^{(1)}(k|k') P(k') \frac{k'}{\overline{k}} = \frac{\overline{k(k-1)^2}}{\overline{k}}. \quad (40)$$

$$\sum_{kk'} c_k (k-1)(k'-1) P^{(1)}(k|k') P(k') \frac{k'}{\overline{k}} = \frac{\overline{k(k-1)^2 c_k}}{\overline{k}}. \quad (41)$$

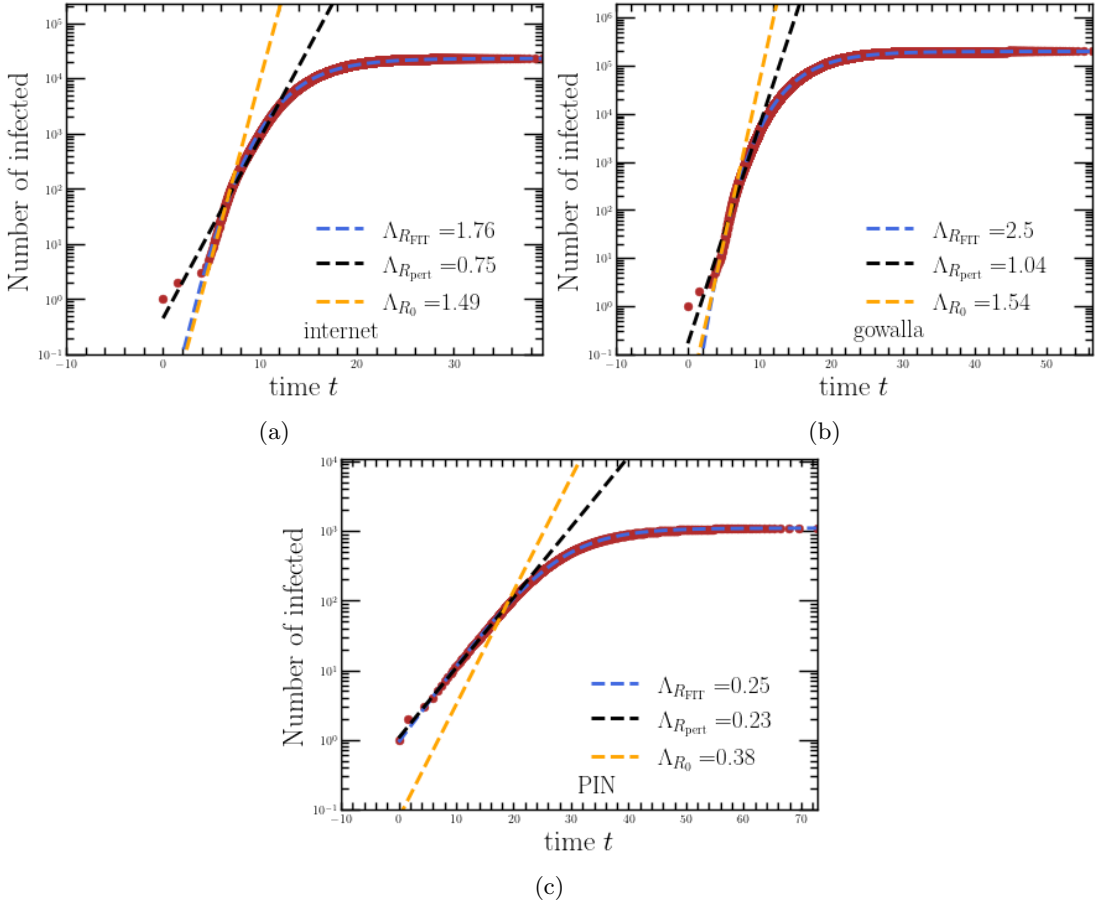


FIG. 25: **Illustration of the difference between  $R_{\text{pert}}$  and  $R_0$  for various networks.** We simulate the average epidemic using a lognormal distribution on four different networks: internet (a), gowalla (b) and PIN (c). We compare the difference in the spreading rates using different estimates of the reproduction number. The first two networks do not exhibit a clear exponential regime (internet:  $\eta = 0.13$ , Gowalla:  $\eta = 0.38$ , opposed to PIN:  $\eta = 0.01$ )

$$\sum_{kk'} c_k c_{k'} (k-1)(k'-1) P^{(1)}(k|k') P(k') \frac{k'}{k} = \frac{\overline{k(k-1)^2 c_k}}{\bar{k}}. \quad (42)$$

Eq. (41) and Eq. (42) yield the same result due to degree detailed balance, which holds because links are undirected. Indeed, we have

$$P(k|k') P(k') \frac{k'}{k} = P(k'|k) P(k) \frac{k}{k'} \quad (43)$$

$$\left( \frac{k}{k'} P(k)(1-r) + r(P^{(1)}(k|k')) \right) P(k') \frac{k'}{k} = \left( \frac{k'}{k} P(k')(1-r) + r(P^{(1)}(k'|k)) \right) P(k) \frac{k}{k'} \quad (44)$$

$$P(k') \frac{k'}{k} \frac{k}{k'} P(k)(1-r) + r(P^{(1)}(k|k') P(k') \frac{k'}{k}) = P(k) \frac{k}{k'} \frac{k'}{k} P(k')(1-r) + r(P^{(1)}(k'|k) P(k) \frac{k}{k'}) \quad (45)$$

$$P^{(1)}(k|k') P(k') \frac{k'}{k} = P^{(1)}(k'|k) P(k) \frac{k}{k'}. \quad (46)$$

The fourth term in the sum reads

$$\sum_{kk'} c_k c_{k'} (k-1)(k'-1) P^{(1)}(k|k') P(k') \frac{k'}{k}. \quad (47)$$

To evaluate this sum, we first make use of the fact that:

$$c_k (k-1) = \sum_{k'} m_{kk'} P(k'|k). \quad (48)$$



This relation holds for any network [7]. Since Eq. (48) is valid for any network, it also holds when  $m_{kk'}$  factorises, i.e, when  $m_{kk'} = c_k(k-1)c_{k'}(k'-1)/m_1$ . We then write Eq. (48) as

$$(k-1)c_k = \frac{1}{m_1} \sum_{k'} c_k(k-1)c_{k'}(k'-1)P(k'|k) \quad (49)$$

$$m_1 = \sum_{k'} c_{k'}(k'-1)P(k'|k) \quad (50)$$

$$m_1 = (1-r) \sum_{k'} c_{k'}(k'-1) \frac{k'}{\bar{k}} P(k') + r \sum_{k'} c_{k'}(k'-1)P^{(1)}(k'|k) \quad (51)$$

$$m_1 = (1-r)m_1 + r \sum_{k'} c_{k'}(k'-1)P^{(1)}(k'|k) \quad (52)$$

$$\implies \sum_{k'} c_{k'}(k'-1)P^{(1)}(k'|k) = m_1. \quad (53)$$

Thus, we express the last term as

$$\sum_{kk'} c_k(k-1)c_{k'}(k'-1)P^{(1)}(k|k')P(k') \frac{k'}{\bar{k}} = m_1^2. \quad (54)$$

Therefore, we write the leading eigenvalue as

$$R_{\text{pert}} = R_{\text{unper}}(1-r) + \frac{r}{R_{\text{unper}}} \left( \frac{\overline{k(k-1)^2}}{\bar{k}} - 2m_2 + m_1^2 \right) + \mathcal{O}(r^2), \quad (55)$$

where we identify  $m_2 = \overline{k(k-1)^2 c_k / \bar{k}}$ .

We remark that  $m_2$  is indirectly related to the average degree of nodes being part of a triangle. After picking randomly a triangle in the network, we pick one of the three nodes. The probability that it has degree  $k$  is given by  $c_k(k-1)kP(k)/(m_1\bar{k})$ . Thus the average degree of a node belonging to a triangle is expressed by

$$\sum_k \frac{c_k(k-1)}{m_1} \frac{k^2}{\bar{k}} P(k) = \sum_k \frac{c_k(k-1)^2}{m_1} \frac{k}{\bar{k}} P(k) + \sum_k \frac{c_k(k-1)}{m_1} \frac{k}{\bar{k}} P(k) \quad (56)$$

$$= \frac{m_2}{m_1} + 1. \quad (57)$$

Finally, the first order correction of the right eigenvector associated to the unique leading eigenvalue is given by

$$v_k^{(1)} = v_k^{(0)} + \frac{r}{R_{\text{unper}}} \sum_{k'} \delta M_{kk'} v_{k'}^{(0)} + \mathcal{O}(r^2). \quad (58)$$

$$\sum_{k'} \delta M_{kk'} v_{k'}^{(0)} = \sum_{k'} (k'-1)(1-c_{k'})P^{(1)}(k|k') \frac{k'}{\bar{k}} P(k') - \sum_{k'} (k'-1)(1-c_{k'})P(k')P(k) \frac{kk'}{\bar{k}^2} \quad (59)$$

$$= \sum_{k'} (k'-1)(1-c_{k'})P^{(1)}(k'|k) \frac{k}{\bar{k}} P(k) - R_{\text{unper}} \frac{k}{\bar{k}} P(k) \quad (60)$$

$$= (k-1) \frac{k}{\bar{k}} P(k) - m_1 \frac{k}{\bar{k}} P(k) - R_{\text{unper}} \frac{k}{\bar{k}} P(k). \quad (61)$$

Therefore, we obtain

$$v_k^{(1)} = (1-r) \frac{k}{\bar{k}} P(k) + \frac{r}{R_{\text{unper}}} ((k-1) - m_1) \frac{k}{\bar{k}} P(k) + \mathcal{O}(r^2). \quad (62)$$

## VI. ESTIMATING THE TAIL OF THE DEGREE DISTRIBUTION

We say that a degree distribution follows a pure power law if it is of the form

$$P(k) = ck^{-\gamma}, \quad c > 0, \gamma > 0. \quad (63)$$

However, real-world data are often better fit by other distributions [12], such as a lognormal. Not even the degree distribution of the Barabási-Albert model follows a pure power law [6], although it is considered as the emblematic model of power-law degree distributions.

We say that a degree distribution is heavy-tailed if it can be expressed in the form:

$$P(k) = \ell(k)k^{-\gamma}, \quad (64)$$

where  $f(k)$  is a slowly varying function, i.e. a function which satisfies

$$\lim_{k \rightarrow \infty} \frac{f(xk)}{f(k)} = 1. \quad (65)$$

This definition generalises the concept of scale-free networks beyond pure power-law degree distributions. Our goal is to determine the exponent  $\gamma$  when the degree distribution has the form of Eq. (64). We follow the method in [13]. Rather than directly estimating  $\gamma$ , the methods estimates the parameter  $\xi = (\gamma - 1)^{-1}$ , which can be interpreted as an extreme value index. When  $\xi > 0$ ,  $P(k)$  is a heavy-tailed distribution and its exponent  $\gamma$  is given by  $\gamma = 1 + 1/\xi$ . There exist various methods to estimate  $\xi$  in a consistent way [13]. From a public software [14], we use the kernel estimator [15], which we observed to capture well the tail of the degree distribution. When the kernel method fails, we use the method of moments. We provide the values of  $\gamma$  estimated with different methods for all real networks in Table IX.

TABLE IX: Exponent of the tail of the degree distribution for real networks.

Network	$\gamma_{\text{hill}}$	$\gamma_{\text{moments}}$	$\gamma_{\text{kernel}}$
amazon	3.68	3.43	3.71
asCaida	2.12	2.11	2.13
asOregon	2.07	2.12	2.12
asSkitter	2.38	2.36	2.44
astroPh	4.46	5.68	7.36
brightkite	3.50	3.80	2.96
condMat	3.66	4.09	4.01
DBLP	6.54	14.89	3.09
deezerEurope	4.91	5.01	5.56
deezerHR	4.67	22.17	5.93
deezerHU	5.43	-89.82	7.63
deezerRO	4.98	8.13	5.46
douban	4.40	9.39	7.11
email	12.58	3.38	2.13
fbArtist	3.15	3.18	3.05
fbAthletes	3.24	3.71	56.00
fbCompany	3.51	3.76	4.00
fbNewSites	3.27	3.70	81.76
fbPublicFigures	9.50	-2.03	3.03
github	2.55	2.53	2.56
gowalla	2.81	2.79	2.86
internet	2.08	2.10	2.10
lastfm	3.76	3.90	3.57
liveJournal	3.60	4.09	3.31
livemocha	7.04	-5.77	2.38
museaFacebook	3.35	3.71	3.85
pgp	4.11	4.40	4.48
PIN	3.12	3.53	3.61
powergrid	7.44	7.63	9.14
roadCA	18.79	-1.56	3.27
roadPA	18.30	-1.65	3.35
roadTX	21.66	-1.42	7.16
twitch	2.54	2.56	2.67
wordnet	28.76	2.67	2.60
youtube	2.48	2.58	2.17

TABLE X: Comparison of  $\gamma$  values for different networks

- 
- [1] Cohen, R., Erez, K., Ben-Avraham, D. & Havlin, S. Resilience of the internet to random breakdowns. *Physical Review Letters* **85**, 4626 (2000).
- [2] Newman, M. E. Spread of epidemic disease on networks. *Physical Review E* **66**, 016128 (2002).
- [3] Noh, J. D. Percolation transition in networks with degree-degree correlation. *Physical Review E* **76**, 026116 (2007).
- [4] Pigolotti, S. Generalized Euler-Lotka equation for correlated cell divisions. *Physical Review E* **103**, L060402 (2021).
- [5] Glynn, P. W. & Whitt, W. Large deviations behavior of counting processes and their inverses. *Queueing Systems* **17**, 107–128 (1994).
- [6] Pósfai, M. & Barabási, A.-L. *Network Science* (Citeseer, 2016).
- [7] Serrano, M. A. & Boguná, M. Tuning clustering in random networks with arbitrary degree distributions. *Physical Review E* **72**, 036133 (2005).
- [8] Leskovec, J. & Krevl, A. SNAP Datasets: Stanford large network dataset collection. <http://snap.stanford.edu/data> (2014).
- [9] Clauset, A., Tucker, E. & Sainz, M. The Colorado Index of Complex Networks. <https://icon.colorado.edu/> (2016).
- [10] Kunegis, J. KONECT – The Koblenz Network Collection. In *Proc. Int. Conf. on World Wide Web Companion*, 1343–1350 (2013). URL <http://dl.acm.org/citation.cfm?id=2488173>.
- [11] Gibson, M. A. & Bruck, J. Efficient exact stochastic simulation of chemical systems with many species and many channels. *The journal of physical chemistry A* **104**, 1876–1889 (2000).

- [12] Broido, A. D. & Clauset, A. Scale-free networks are rare. *Nature Communications* **10**, 1017 (2019).
- [13] Voitalov, I., Van Der Hoorn, P., Van Der Hofstad, R. & Krioukov, D. Scale-free networks well done. *Physical Review Research* **1**, 033034 (2019).
- [14] Voitalov, I. Tail index estimation for degree sequences of complex networks. <https://github.com/ivanvoitalov/tail-estimation> (2018).
- [15] Groeneboom, P., Lopuhaä, H. P. & De Wolf, P. Kernel-type estimators for the extreme value index. *The Annals of Statistics* **31**, 1956–1995 (2003).